Rubio, L., Fernández-Sáez, J., Morassi, Antonio. (2015). Crack identification in non-uniform rods by two frequency data. *International Journal of Solids and Structures,* 75-76, pp. 61-80.

DOI:10.1016/j.ijsolstr.2015.08.001

Crack identification in non-uniform rods by two frequency data

Lourdes Rubio [a], José Fernández-Sáez [b], Antonino Morassi [c,*]

[a] Department of Mechanical Engineering, University Carlos III of Madrid, Avda. de la Universidad 30, 28911 Leganés, Madrid, Spain
[b] Department of Continuum Mechanics and Structural Analysis, University Carlos III of Madrid, Avda. de la Universidad 30, 28911 Leganés, Madrid, Spain
[c] Università degli Studi di Udine, Dipartimento di Ingegneria Civile e Architettura, via Cotonificio 114, 33100 Udine, Italy

A B S T R A C T

We consider the inverse problem of identifying a single open crack in a longitudinally vibrating rod hav-ing non-uniform smooth profile. Without any a priori assumption on the smallness of the damage and assuming that the rod profile is symmetric with respect to the mid-point of the rod axis, we present a constructive diagnostic algorithm from minimal frequency data. We show that the crack can be uniquely identified, up to a symmetric position, from the first two positive natural frequencies of the rod under free–free end conditions. We also show that the non-uniqueness of the damage location can be removed by using as data the first positive resonant frequency of the free–free rod and the first antiresonant fre-quency of the driving-point frequency response evaluated at one end of the rod. The results of numerical simulations and of applications of the method to experimental data agree well with the theory.

Keywords:
Damage identification, Non-uniform rods Cracks, Natural frequencies, Antiresonant frequencies, Inverse problems

1. Introduction

Non-uniform vibrating beams are frequently used in engineering applications since they may offer the advantage for a selective distribution of stiffness and mass. This may help in fitting special design requirements and in obtaining optimal dynamical responses.

In spite to the importance of the vibrational behavior of such beams, many studies focussed on uniform beams. The lack of research is all the greater in the case of non-uniform beams with a localized damage, such as a crack, and, particularly, on the inverse problem of identifying the damage from dynamic data. Actually, several researchers considered the identification of a single (open) crack from frequency measurements, but their studies were often restricted to rods with uniform profile, see, among others, the contributions (Springer et al., 1988; Lin and Chang, 2004; Rubio, 2009; Cerri and Vestroni, 2000; Vestroni and Capecchi, 2000). A limited number of researches focussed on crack identification on non-uniform beams. We refer, for example, to the paper Chaudhari and Maiti (2000) for a study of direct and inverse problems for geometrically segmented cracked beams, and to the contributions Adams et al. (1978) and Liang et al. (1992) for resonant frequency-based damage assessment in tapered and piecewise constant cracked beams, respectively.

In this paper we shall concern with the crack identification problem for beams under longitudinal vibrations (rods) by minimal spectral data. One of the first rigorous results on this topic is due to Narkis (1994), who proved that a single small crack in a free–free uniform rod can be uniquely localized (up to a symmetric position) by the first two positive natural frequencies of the longitudinal vibration. Under the assumption that the crack remains open during vibration, the damage was modeled as a translational linearly elastic spring, of stiffness K, located at the cross-section of abscissa s. The stiffness value K can be estimated in terms of the geometry of the cross-section and the mechanical properties of the beam, see Freund and Herrmann (1976). An extended series of experiments confirm the accuracy of the localized flexibility model for cracked rods, particularly for low frequencies, see, among other contributions, Caddemi and Morassi (2013). Narkis's method is based on a perturbation analysis and takes advantage of the fact that the frequency equation for a uniform cracked rod can be written in explicit form.

The identification of a single small crack in a rod with variable profile has been considered in Morassi (2001). Working directly on the weak formulation of the eigenvalue problem, it was shown in Morassi (1993) that the first order change $\delta\lambda_n$ in a generic eigenvalue λ_n (e.g., the resonant frequency squared) is given by

$$\delta\lambda_n = \frac{N_n^2(s)}{K}, \tag{1}$$

where $N_n(s)$ is the axial force in the nth vibration mode of the undamaged rod, evaluated at the cracked cross-section of abscissa s. It follows that the ratio of the first order changes to two eigenvalues

$$\frac{\delta\lambda_n}{\delta\lambda_m} = \frac{N_n^2(s)}{N_m^2(s)} \tag{2}$$

is known as a function of s only, and it may be possible to find the position of the crack s corresponding to a given (measured) value of $\frac{\delta\lambda_n}{\delta\lambda_m}$. In particular, for a free–free rod with regular profile $a = a(x)$ (e.g., a continuous and continuously differentiable function) and symmetric with respect to the mid-point, it was shown in Morassi (2001) that the knowledge of the first ($m = 1$) and second ($n = 2$) positive eigenfrequencies uniquely determines the position of the crack, up to a symmetric position. Under the same assumptions, the indeterminacy induced by the symmetry of the rod can be removed by using the first resonant frequency of the free–free rod and the first antiresonant frequency of the driving point frequency response function measured at one end of the rod, see Dilena and Morassi (2004).

All the results found in Narkis (1994), Morassi (2001) and Dilena and Morassi (2004) hold under the essential hypothesis that the severity of the crack is small, that is the cracked rod is a perturbation of the undamaged rod. In addition, it should be noticed that the identification algorithm proposed in Morassi (2001) and Dilena and Morassi (2004) is constructive for rods with uniform profile only. The assumption of light damage is reasonable in many practical applications. However, it is not easy to state rigorously when a crack can be considered as small. In fact, even restricting the analysis to the linearized frequency change, Eq. (1) shows that the vibration modes have wavy sensitivity to damage according to the position of the crack, and that the wavy character is more oscillating as the mode order increases. The introduction of an average frequency shift does not simplify the analysis, since it should be clarified how many data must be included in the calculation and how the threshold value corresponding to small damage should be selected. In addition, it is desirable to obtain a unifying general theory of the diagnostic problem capable to include damages ranging from small to large severity.

A first rigorous attempt to solve the inverse problem of detecting a not necessarily small crack in a rod has been presented in Rubio et al. (2015). The authors have shown that the results found in Morassi (2001) and Dilena and Morassi (2004) for a small crack continue to hold even for a crack with any level of severity, provided that the rod is uniform. The proof presented in Rubio et al. (2015) is based on a careful analysis of the solutions of the nonlinear system formed by the frequency equation (which is available in closed form) written for the pair of spectral input data, together with suitable lower and upper bounds derived within the variational theory of eigenvalues.

When a rod has variable profile, no closed form expression for the frequency equation is available and a different approach must be adopted for the identification of damage. This open inverse problem has motivated our research and its solution is the objective of the present study. The main steps of our analysis are as follows.

(i) We introduce an equivalent problem for a vibrating rod with a point mass m at the position s.
(ii) We determine the qualitative behavior of the so called $\lambda - m$ and $\lambda - s$ curves, that is the functions $\lambda_n = \lambda_n(s, \cdot)$ and $\lambda_n = \lambda_n(\cdot, m)$, for fixed s and fixed m, respectively.
(iii) We solve the inverse problem by combining the information contained in the $\lambda - m, \lambda - s$ curves corresponding to the pair of frequency data used in identification.

Let us illustrate with some more details the content of such steps.

Step (i) is based on a transformation of the eigenvalue problem for the cracked rod in an equivalent eigenvalue problem for a rod with a point mass $m = \frac{1}{K}$ located at the cracked cross-section, with suitable coefficients and under proper boundary conditions (see Proposition 2.1 for a precise statement). Therefore, the problem of identifying the crack is transformed in the equivalent problem of determining the location and magnitude of the point mass from a pair of natural frequencies.

Step (ii) is mainly based on the explicit determination of the eigenvalue derivatives with respect to the parameters s and m. The expression of the derivative $\frac{\partial\lambda}{\partial m}$ was used in Morassi and Dilena (2002) in a study of the inverse problem of locating a small point mass in a vibrating rod from natural frequency data. The analysis of the $\lambda - m$ and $\lambda - s$ curves allows to determine the qualitative behavior of the first and second eigenvalue of the free–free rod with respect to the position and intensity of the point mass (see Theorem 5.5 for details). It is exactly at this point that, for technical reasons, we restrict the attention to rods having symmetric profile with respect to the mid-point of the axis.

The results obtained in Step (ii) and the use of suitable general properties of the eigenpairs of the problem, allowed to develop in Step (iii) a reconstruction algorithm for the identification of the point mass (up to a symmetric location) from the first two positive resonant frequencies of the rod. An extended series of numerical simulations on rods having different profile and for various positions and intensities of the crack supported the theoretical results. A selected set of numerical results and some applications to experimental data are presented in Section 9.

The above results can be generalized in a couple of directions. First, the crack identification problem can be formulated and solved in terms of resonant and antiresonant data (see Section 7), thus showing that both the severity and the location of the crack can be uniquely determined by measuring the first positive natural frequency under free–free end conditions and the first antiresonant frequency of the driving frequency response evaluated at one end of the rod. Second, the analysis can be carried out also for symmetric rods in which the linear mass density is not proportional to the axial stiffness function (see Section 8).

The paper is organized as follows. The reduction of the eigenvalue problem for the cracked rod to an equivalent eigenvalue problem for a rod with a point mass is shown in Section 2. Certain basic properties of the eigenvalue problem for the rod with a point mass are listed in Section 3. The first order partial derivatives of an eigenvalue with respect to the point mass and the mass location are determined in Section 4. The behavior of the λ-m and λ-s curves is studied in Section 5. The damage identification algorithm in a free–free rod based on measurements of the first two positive natural frequencies is presented in Section 6. Generalizations to resonant-antiresonant frequency data and to larger classes of rods are illustrated in Section 7 and Section 8, respectively. Section 9 is devoted to numerical and experimental applications of the theory. Proofs of some technical results are collected in Appendix (Section A). We think that the disadvantage of increasing the size of the paper by including the Appendix is by far out-weighed by the fact that Section 3 and, partially, Section 5, together with the Appendix, represent a self-contained approach to the topic.

2. An equivalent eigenvalue problem for a rod with a point mass and main result

Let us consider a longitudinally vibrating free–free straight thin rod of length L. Denote by $\widehat{A} = \widehat{A}(z)$ the area of the transversal

cross-section of the rod, $z \in [0, L]$, and assume that $\widehat{A}$ is a strictly positive, continuously differentiable function in $[0, L]$. The (constant) Young's modulus of the material is denoted by $E, E > 0$; γ is the (uniform) volume mass density, $\gamma > 0$. We assume that the rod has a single crack at the cross-section of abscissa z_d, with $0 < z_d < L$. The crack is assumed to remain open during vibration and it is modeled as a longitudinal linearly elastic spring with stiffness $\widehat{K}$, see, for example, Freund and Herrmann (1976) and Cabib et al. (2001). The value of $\widehat{K}$ depends on the geometry of the cracked cross-section and on the material properties of the beam, see Section 9 for a specific expression in the case of rectangular cross-section and transversal cracks. The free undamped longitudinal vibrations of the rod with radian frequency ω and spatial amplitude $\hat{u} = \hat{u}(z)$ are governed by the following eigenvalue problem

$$\begin{cases} \dfrac{d}{dz}\left(E\hat{A}(z)\dfrac{d\hat{u}(z)}{dz}\right) + \omega^2\gamma\hat{A}(z)\hat{u}(z) = 0, \quad z \in (0, z_d) \cup (z_d, L), & (3)\\ [[E\hat{A}(z_d)\dfrac{d\hat{u}}{dz}(z_d)]] = 0, & (4)\\ \hat{K}[[\hat{u}(z_d)]] = E\hat{A}(z_d)\dfrac{d\hat{u}}{dz}(z_d), & (5)\\ E\hat{A}(0)\dfrac{d\hat{u}}{dz}(0) = 0 = E\hat{A}(L)\dfrac{d\hat{u}}{dz}(L), & (6) \end{cases}$$

where $[[\hat{u}(z_d)]] = \lim_{z \to z_d^+}\hat{u}(z) - \lim_{z \to z_d^-}\hat{u}(z)$.

By introducing the change of variables

$$x = \frac{z}{L} \tag{7}$$

and defining

$$u(x) = \hat{u}(z), \quad A(x) = \hat{A}(z), \quad a(x) = \frac{A(x)}{A(x_0)} \text{ for a given } x_0 \in [0, 1], \tag{8}$$

the eigenvalue problem (3)–(6) can be written in dimensionless form as

$$\begin{cases} (au')' + \lambda au = 0, \quad x \in (0, s) \cup (s, 1), & (9)\\ [[au'(s)]] = 0, & (10)\\ K[[u(s)]] = a(s)u'(s), & (11)\\ a(0)u'(0) = 0 = a(1)u'(1), & (12) \end{cases}$$

where

$$s = \frac{z_d}{L} \in (0, 1), \quad K = \frac{\hat{K}L}{EA(x_0)} \in (0, \infty), \quad \lambda = \frac{\gamma L^2\omega^2}{E}. \tag{13}$$

Hereinafter, we use the notation $(\cdot)' = \frac{d(\cdot)}{dx}$ to indicate x-differentiation. Note that the dimensionless area of the transversal cross-section of the rod $a = a(x)$ is a strictly positive, continuously differentiable function of x in $[0, 1]$.

Under the above assumptions, there exists a numerable sequence of real, non-negative eigenvalues $\{\lambda_n\}_{n=0}^{\infty}$ of (9)–(12) with accumulation point at ∞. This property follows from standard results for self-adjoint compact operators in an Hilbert space, see, for example, Brezis (1986), Courant and Hilbert (1966). Note that the lower eigenvalue $\lambda_0 = 0$ corresponds to a rigid body motion $u(x) = const$.

In order to study the eigenvalue problem (9)–(12), we find convenient to introduce an equivalent problem. The equivalence is stated in the next proposition. Let u be a non-trivial solution of (9)–(12) for an eigenvalue λ. We denote by (λ, u) the corresponding eigenpair.

Proposition 2.1.

(i) *Let (λ, u) be an eigenpair of (9)–(12). If $\lambda > 0$, then λ is an eigenvalue of the problem*

$$\begin{cases} (bw')' + \lambda bw = 0, \quad x \in (0, s) \cup (s, 1), & (14)\\ [[w(s)]] = 0, & (15)\\ [[bw'(s)]] = -\lambda m w(s), & (16)\\ w(0) = 0 = w(1), & (17) \end{cases}$$

with

$$w = au' \quad in\ (0, s) \cup (s, 1), \quad b = a^{-1} \quad in\ \in [0, 1], \quad m = K^{-1}. \tag{18}$$

(ii) Conversely, if (λ, w) is an eigenpair of the problem (14)–(17), then $\lambda, \lambda > 0$, is an eigenvalue of the problem (9)–(12) with eigenfunction u such that

$$u = bw' \quad in\ (0, s) \cup (s, 1), \quad a = b^{-1} \quad in\ (0, 1), \quad K = m^{-1}. \tag{19}$$

Proof.

(i) Using (18) in (9), dividing by a and differentiating, we obtain

$$\left(\frac{w'}{a}\right)' + \lambda\frac{w}{a} = 0, \quad x \in (0, s) \cup (s, 1), \tag{20}$$

which is (14) for $b = a^{-1}$. The end conditions (17) and the jump condition (15) follow immediately by the definition of w and by (10), (12). In order to deduce (16), we use (9) to determine the limit values $bw'(s^{\pm})$ and jump condition (11):

$$[[bw'(s)]] = -\lambda[[u(s)]] = -\frac{\lambda}{K}w(s). \tag{21}$$

(ii) The proof follows the same steps of the proof of case (i). □

Remark 2.2. The eigenvalue problem (14)–(17) describes the free, undamped longitudinal vibrations of a rod with cross-sectional area $b = b(x)$, b being a strictly positive and continuously differentiable function in $[0, 1]$, under simply supported end conditions and with a point mass m placed at $x = s, 0 < m < \infty$.

In the sequel, basing on the equivalence between the eigenvalue problems (9)–(12) and (14)–(17) established in Proposition 2.1, we will mainly consider the formulation in terms of the vibration of the rod with the point mass. It should be noted that there is an advantage connected with this choice, namely, the functional space in which the eigenvalue problem (14)–(17) is formulated is formed by functions that are more regular than those involved in (9)–(12). In fact, jump of an eigenfunction w at $x = s$ is not allowed, whereas the eigenfunction u may be discontinuous at the crack location. This additional regularity simplifies the analysis of the general properties of the eigenvalue problem (see Section 3) and the study of the dependence of the eigenvalue on the damage variables s and K (see Sections 4 and 5).

Taking the above considerations into account, our main result on crack identification in a longitudinally vibrating rod under free–free end conditions can be rephrased as follows.

Theorem 2.3. *Let $b = b(x)$ a strictly positive and continuously differentiable function in $[0, 1]$, with $b(x) = b(1 - x)$. The measurement of the first two natural frequencies of (14)–(17) allows for the unique determination of the intensity m and the location s of the point mass, up to the symmetric position $(1 - s)$. The identification procedure is constructive.*

Sections 3–6 are devoted to the proof of Theorem 2.3. As we premised in the Introduction, the proof consists of several steps. Some qualitative properties of the eigenvalue problem (14)–(17),

which play an important role in the inverse problem, are collected in Section 3. The study of the λ-m and λ-s curves for the first two eigenvalues is developed in Sections 4 and 5. It should be noted that the assumption of symmetrical profile, e.g., $b(x) = b(1-x)$ in $[0,1]$, was introduced exactly in this part in order to prove some specific properties of the critical points of the λ-s curves. Finally, the above results are used in Section 6 to prove the main theorem by means of a constructive procedure.

3. Qualitative properties of the eigenvalue problem

In this section, the qualitative properties of the eigenvalue problem (14)–(17) useful in our analysis are recalled. Most of them are obtained as generalization of the corresponding results for classical Sturm–Liouville eigenvalue problems (e.g., with $m = 0$) (Gladwell, 2004). For the sake of completeness and for reader's convenience, essential details of the proofs are presented in Appendix.

Proposition 3.1. *The eigenvalues of* (14)–(17) *are all simple.*

For a proof we refer to Appendix (Section A.1). It follows that the spectrum of (14)–(17) is made by a strictly increasing sequence of real numbers

$$0 < \lambda_1 < \lambda_2 < \dots, \tag{22}$$

and to each eigenvalue we can associate a unique eigenfunction, as it is stated in the following simple consequence of Proposition 3.1.

Corollary 3.2. *Let w and $\widetilde{w}$ be eigenfunctions of* (14)–(17) *associated to the same eigenvalue λ. Then*

$$w = c\widetilde{w}, \quad \text{in } [0,1], \tag{23}$$

where c is a non-vanishing constant.

Weak and variational formulation of the eigenvalue problem (14)–(17) will be used in several places throughout the paper. The weak formulation consists in finding $w \in H_0^1(0,1) \setminus \{0\}$ such that

$$\int_0^1 bw'\varphi' = \lambda\left(\int_0^1 bw\varphi + mw(s)\varphi(s)\right), \quad \text{for every } \varphi \in H_0^1(0,1). \tag{24}$$

Here, $H_0^1(0,1)$ is the Hilbert space of Lebesgue measurable functions $f : (0,1) \to \mathbb{R}$ such that f and its first weak derivative, f', are square summable in $(0,1)$, e.g., $\int_0^1 f^2 + \int_0^1 (f')^2 < \infty$, and the trace of f at $x = 0$ and $x = 1$ vanishes, e.g., $f(0) = f(1) = 0$.

The Rayleigh's Quotient associated to (24) is

$$R[\cdot] : H_0^1(0,1) \setminus \{0\} \to \mathbb{R}, \quad R[\varphi] = \frac{\int_0^1 b(\varphi')^2}{\int_0^1 b\varphi^2 + m\varphi^2(s)}. \tag{25}$$

Within the variational formulation of (14)–(17) the eigenvalues are determined by solving the chain of minimum problems

$$R[w_n] = \min_{\varphi \in V_n \setminus \{0\}} R[\varphi] = \lambda_n, \tag{26}$$

where

$$V_n = \left\{ \varphi \in H_0^1(0,1) \text{ s.t. } \int_0^1 bw_i\varphi + mw_i(s)\varphi(s) = 0,\ i = 1,\dots,n-1 \right\}. \tag{27}$$

An alternative, equivalent formulation of the eigenvalue problem (26) and (27) comes from the Maximum–Minimum Principle, that is

$$\lambda_n = \max_{l_i \in (H_0^1(0,1))',\ i=1,\dots,n-1} \left\{ \min_{\varphi \in H_0^1(0,1)\setminus\{0\},\ l_i(\varphi)=0,\ i=1,\dots,n-1} R[\varphi] \right\}, \tag{28}$$

where $(H_0^1(0,1))'$ is the dual space of $H_0^1(0,1)$, that is the space of all the linear and continuous real-valued functionals l_i on $H_0^1(0,1)$. We refer to Weinberger (1965) for a complete account of the above formulations.

The task of counting the zeros of an eigenfunction of (14)–(17) is solved by the next proposition.

Proposition 3.3. *The nth eigenfunction of* (14)–(17), $n \geqslant 1$, *has exactly $n-1$ zeros inside* $(0,1)$.

A proof of this proposition is presented in Appendix (Section A.2).

In the next sections we shall often compare the eigenpairs of the problem (14)–(17) for finite no-vanishing m and $s \in (0,1)$, to those obtained by taking either $m = 0$ or $\{s = 0, s = 1\}$ in (14)–(17). For this reason, we shall denote by (λ_n^U, w_n^U) the nth eigenpair of the so-called *unperturbed* problem

$$\begin{cases} (bw^{U'})' + \lambda^U bw^U = 0, & x \in (0,1), \quad (29) \\ w^U(0) = 0 = w^U(1). & \quad (30) \end{cases}$$

Accordingly, the eigenpairs of the problem (14)–(17) will be called *perturbed* in the following. Clearly, there exists a numerable sequence of real, simple, strictly positive eigenvalues of (29) and (30), say $0 < \lambda_1^U < \lambda_2^U < \dots$, with $\lim_{n\to\infty} \lambda_n^U = \infty$. Weak, variational and Maximum–Minimum formulation of (29) and (30) can be deduced by (24), (26)–(28), respectively, taking formally $m = 0$. Note that the statement of Proposition 3.3 obviously hold also for the unperturbed problem.

By the variational and Maximum–Minimum formulation, the following eigenvalue bounds can be deduced.

Proposition 3.4. *Under the above assumptions and notation, we have*

$$\lambda_{n-1}^U \leqslant \lambda_n \leqslant \lambda_n^U, \quad \text{for every } n \geqslant 1, \tag{31}$$

where we have defined $\lambda_0^U = 0$.

Weak and variational formulations are powerful tools, but they are not completely helpful in answering some of the questions that interest us, particularly the quantitative dependence of an eigenvalue to the perturbation parameters m and s. For this reason, in the next section we shall introduce the first-order partial derivatives of an eigenvalue of (14)–(17) with respect to m and s, and we begin the study of the function $\lambda_n = \lambda_n(s,m)$.

4. Eigenvalue derivatives

For a given, strictly positive continuously differentiable coefficient b, the eigenpair (λ, w) of (14)–(17) depends on the perturbation parameters s and m. When necessary, we shall explicitly show this dependence by writing $\lambda = \lambda(s,m)$ and $w = w(x;s,m)$, where x is the current spatial variable ranging from 0 to 1. In some cases, to simplify the notation and when there is no ambiguity, we shall omit the explicit dependence on the perturbation parameters.

Proposition 4.1. *Let (λ, w) be an eigenpair of* (14)–(17). *We have*

$$\frac{\partial\lambda}{\partial s} = -\lambda\, \frac{mw(s)(w'(s^+) + w'(s^-))}{mw^2(s) + \int_0^1 bw^2}, \tag{32}$$

$$\frac{\partial\lambda}{\partial m} = -\lambda\, \frac{w^2(s)}{mw^2(s) + \int_0^1 bw^2}, \tag{33}$$

where

$w'(s^+) = \lim_{x_0 \to s^+} \left(\frac{dw(x;s,m)}{dx}|_{x=x_0}\right)$, $w'(s^-) = \lim_{x_0 \to s^-} \left(\frac{dw(x;s,m)}{dx}|_{x=x_0}\right)$.

Proof. The authors are indebted with Giovanni Alessandrini for providing the proof of (32).

By (24), let us rewrite the eigenvalue problem (14)–(17) in weak form: to find $w \in H_0^1(0,1) \setminus \{0\}$ such that

$$\int_0^1 bw'\varphi' = \lambda\left(mw(s)\varphi(s) + \int_0^1 bw\varphi\right), \quad \text{for every } \varphi \in H_0^1(0,1). \tag{34}$$

By density results, it is enough to take φ in the set of C^1-piecewise functions in $[0,1]$, with $\varphi(0) = \varphi(1) = 0$. Therefore, φ has finite left and right first derivative at every point of $(0,1)$, and $\varphi'(0^+)$ and $\varphi'(1^-)$ there exist and are finite. Let us introduce the operator

$$\Delta_h f(s) = \frac{f(s+h) - f(s)}{h}, \quad h > 0,\ s \in [0, 1-h]. \tag{35}$$

We apply Δ_h to (34) obtaining

$$\begin{aligned}\int_0^1 b(\Delta_h w')\varphi' =& \Delta_h\lambda\left(mw(s)\varphi(s) + \int_0^1 bw\varphi\right)\\ &+ \lambda\left(m\Delta_h(w(s)\varphi(s)) + \int_0^1 b(\Delta_h w)\varphi\right)\end{aligned} \tag{36}$$

where here φ is any test function (given independently from the position s of the point mass). We have

$$\begin{aligned}\Delta_h(w(s)\varphi(s)) &= \frac{1}{h}(w(s+h)\varphi(s+h) - w(s)\varphi(s))\\ &= \frac{1}{h}((w(s+h) - w(s))\varphi(s)\\ &\quad + w(s+h)(\varphi(s+h) - \varphi(s)))\\ &= (\Delta_h w(s))\varphi(s) + w(s+h)\Delta_h(\varphi(s)).\end{aligned} \tag{37}$$

Recalling that $w(s) = w(x = s; s)$ (here the dependence on the mass intensity m is omitted), by Lagrange's theorem we have

$$\begin{aligned}\Delta_h w(s) &= \frac{1}{h}(w(s+h; s+h) - w(s; s))\\ &= \frac{1}{h}(w(s+h; s+h) - w(s; s+h)) + \frac{1}{h}(w(s; s+h) - w(s; s))\\ &= w'(s+\zeta_h; s+h) + \Delta_h(w(z; s)|_{z=s}),\end{aligned} \tag{38}$$

with $0 < \zeta_h < h$. Note that

$$\lim_{h\to 0^+} w'(s+\zeta_h; s+h) = w'(s^-; s), \tag{39}$$

see Fig. 1. Replacing (38) in (37) and in (36), we have

$$\begin{aligned}\int_0^1 b(\Delta_h w')\varphi' =& \Delta_h\lambda\left(mw(s)\varphi(s) + \int_0^1 bw\varphi\right)\\ &+ \lambda[m(w'(s+\zeta_h; s+h)\varphi(s)\\ &+ \Delta_h(w(z; s)|_{z=s})\varphi(s)) + mw(s+h)\Delta_h(\varphi(s)) + \int_0^1 b(\Delta_h w)\varphi\Big].\end{aligned} \tag{40}$$

Now, we take $\varphi = w$ and we notice that $\Delta_h w$ belongs to the admissible set of test functions for (34). In fact, $\Delta_h w$ is a piecewise C^1-function in $[0,1]$ and $\Delta_h w(0) = \Delta_h w(1) = 0$. Then, as $h \to 0^+$, by (39) we have

$$\begin{aligned}0 =& \frac{\partial\lambda}{\partial s}(s^+)\left(mw^2(s) + \int_0^1 bw^2\right)\\ &+ \lambda m(w'(s^-; s)w(s; s) + w'(s^+; s)w(s; s)),\end{aligned} \tag{41}$$

and there exists the right derivative

$$\frac{\partial\lambda}{\partial s}(s^+) = -\lambda\,\frac{mw(s)(w'(s^+) + w'(s^-))}{mw^2(s) + \int_0^1 bw^2}. \tag{42}$$

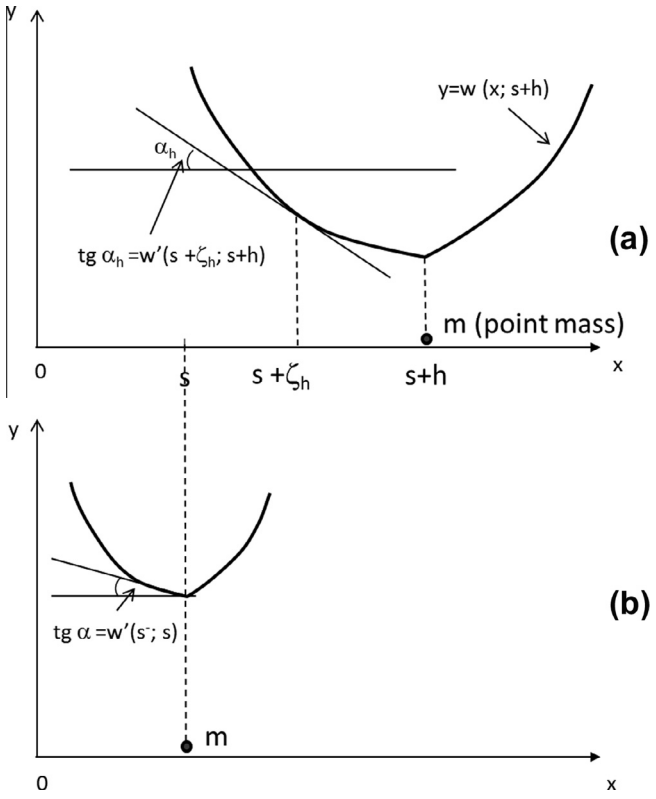

Fig. 1. Left derivative of $w(\cdot; s)$ at s (see Eq. (39)).

Similarly, one can prove that there exists the left derivative $\frac{\partial\lambda}{\partial s}(s^-)$. Left and right derivatives are equal, and (32) is proved.

The proof of (33) is simpler and follows the above arguments. Let us introduce the operator

$$\delta_h f(m) = \frac{f(m+h) - f(m)}{h}, \quad h > 0,\ m \in (0, \infty). \tag{43}$$

We apply the operator δ_h to (34) obtaining

$$\begin{aligned}\int_0^1 b(\delta_h w')\varphi' =& \delta_h\lambda\left(mw(s; m)\varphi(s) + \int_0^1 bw\varphi\right)\\ &+ \lambda\left(w(s; m)\varphi(s) + m(\delta_h w(s; m))\varphi(s) + \int_0^1 b(\delta_h w)\varphi\right),\end{aligned} \tag{44}$$

for every piecewise C^1-function φ defined in $[0,1]$ and such that $\varphi(0) = \varphi(1) = 0$. Here, φ is considered independent from m. We can take $\varphi = w$ in (44). Observing that $\delta_h w$ is an admissible test function for the weak formulation of the eigenvalue problem, (44) becomes

$$0 = \delta_h\lambda\left(mw^2(s; m) + \int_0^1 bw^2\right) + \lambda w^2(s; m). \tag{45}$$

Taking the limit as $h \to 0^+$ we obtain

$$\frac{\partial\lambda}{\partial m}(s; m^+) = -\lambda\,\frac{w^2(s; m)}{mw^2(s; m) + \int_0^1 bw^2}. \tag{46}$$

The left derivative is equal to the right derivative, and (33) is proved. □

5. λ-m and λ-s curves

The identification algorithm presented in Section 6 is based on the properties of the functions $\lambda_n = \lambda_n(s,\cdot)$ and $\lambda_n = \lambda_n(\cdot, m)$, the so-called λ-m and λ-s curves, where λ_n is an eigenvalue of (14)–(17) for a given coefficient b.

We begin with the study of the dependence of λ_n on the parameter m for a given position of the point mass.

Proposition 5.1. *Let $(\lambda_n, w_n), (\lambda_n^U, w_n^U)$ be the nth eigenpair of the problem (14)–(17), (29)–(30), respectively, $n \geqslant 1$.*

(i) If $w_n^U(s_0) = 0$ for some $s_0 \in [0,1]$, then $\lambda_n(s_0, m) = \lambda_n^U$ for every finite positive m.
(ii) If $w_n^U(s_0) \neq 0$ for some $s_0 \in (0,1)$, then $\lambda_n = \lambda_n(s_0, m)$ is a monotonically decreasing function of m in $[0,\infty)$.
(iii) If $\lambda_n(s_0, m_0) = \lambda_n^U$ for some $s_0 \in [0,1]$ and $m_0 \in (0,\infty)$, then $w_n^U(s_0) = 0$.
(iv) If $w_n(s_0; s_0, m_0) = 0$ for some $s_0 \in [0,1]$ and $m_0 \in (0,\infty)$, then $w_n^U(s_0) = 0$.

Proof.

(i) If $w_n^U(s_0) = 0$ for $s_0 \in (0,1)$, then, by direct inspection, w_n^U is an eigenfunction of (14)–(17) with $s = s_0$, for every finite $m > 0$. Precisely, by Proposition 3.3, w_n^U is the eigenfunction associated to the nth eigenvalue $\lambda_n^U = \lambda_n(s_0, m)$. Clearly, the eigenpairs of the unperturbed problem (29)–(30) are insensitive to the point mass either if $s_0 = 0$ or $s_0 = 1$.

(ii) By integrating (33) for a given position s_0 of the mass, $s_0 \in (0,1)$, we get

$$\lambda_n(s_0, m) = \lambda_n^U \exp\left(-\int_0^m \frac{w_n^2(s_0; s_0, t)\,dt}{t w_n^2(s_0; s_0, t) + \int_0^1 b(x) w_n^2(x; s_0, t)\,dx} \right) \tag{47}$$

and the thesis is proved.

(iii) By (47) with $m = m_0$, the condition $\lambda_n(s_0, m_0) = \lambda_n^U$ implies $w_n(s_0; s_0, t) = 0$ for every $t \in (0, m_0)$. Then, since $\lim_{t\to 0^+} w_n(s_0; s_0, t) = w_n^U(s_0)$, the thesis follows.

(iv) If $w_n(x; s_0, m_0)$ is such that $w_n(s_0; s_0, m_0) = 0$, then, by direct inspection in (14)–(17), w_n is an eigenfunction of the unperturbed problem. Precisely, by Proposition 3.3, w_n is the eigenfunction associated to the nth eigenvalue, and $\lambda_n(s_0, m_0) = \lambda_n^U$. By (iii) the thesis follows. □

If the nth eigenvalue of (29)–(30) is sensitive to the point mass, the corresponding eigenmode changes. We compare the nodes (or the zeros) of the corresponding eigenmodes of the problems (29)–(30) and (14)–(17) in the next proposition.

Proposition 5.2. *Suppose that $w_n^U(s) \neq 0$, where $s \in (0,1)$ is the mass position. Then, the nodes of the eigenmodes of the unperturbed rod which are located to the left of s move to the right. Similarly, the nodes to the right of s will move to the left.*

Proof. The proof follows by adapting the proof of the corresponding result derived in Gladwell and Morassi (1999) for longitudinally vibrating rods with a single crack. □

In the remaining part of this section, we shall study the dependence of an eigenvalue of (14)–(17) on the position s of the point mass, for a given finite mass intensity m. We shall study the problem for (initially) *symmetric* rods, that is rods with cross-sectional area $a = a(x)$ which is an even function with respect to the midpoint $x = \frac{1}{2}$, e.g. (after reduction to the equivalent problem by Proposition 2.1)

$$b(1-x) = b(x), \quad x \in [0,1]. \tag{48}$$

A simple consequence of the symmetry of the unperturbed rod is the following proposition.

Proposition 5.3. *Let (λ_n, w_n) be the nth eigenpair of (14)–(17) for b strictly positive, continuously differentiable function satisfying (48). Let m be given, $0 < m < \infty$. Then*

$$\lambda_n(s) = \lambda_n(1-s), \quad s \in [0,1]. \tag{49}$$

If $s = \frac{1}{2}$, then

for n odd, we have $w_n(x) = w_n(1-x)$, (50)

and

for n even, we have $w_n(x) = -w_n(1-x), \quad x \in [0,1]$. (51)

The above statements can be easily verified by direct calculation. Since, by Proposition 4.1, $\lambda_n = \lambda_n(s)$ is a continuously differentiable function, the property (49) implies the following result.

Corollary 5.4. *Under the assumptions of Proposition 5.3, for every $n \geqslant 1$, we have*

$$\dot\lambda_n(s) = 0 \quad \text{for } s \in \left\{0, 1, \frac{1}{2}\right\}. \tag{52}$$

In order to simplify the notation, we have introduced the symbol $\dot\lambda_n$ for the partial derivative of λ_n with respect to s. This notation will be maintained throughout the remaining of the section.

The key result of this section is the following theorem. The result is stated only for the first two eigenvalues of (14)–(17), since only this set of spectral data will be used in Section 6 to identify the point mass.

Theorem 5.5. *Let $(\lambda_n, w_n), n \geqslant 1$, be the nth eigenpair of (14)–(17) for a strictly positive, continuously differentiable function b in $[0,1]$, satisfying (48). Let m be given, $0 < m < \infty$. Then:*

(i) $\lambda_1 = \lambda_1(s)$ is a strictly decreasing function in $(0, \frac{1}{2})$;
(ii) there exists a unique $\widetilde{s} \in (0, \frac{1}{2})$ such that $\dot\lambda_2(\widetilde{s}) = 0$, that is $\lambda_2 = \lambda_2(s)$ is a strictly decreasing function and a strictly increasing function in $(0, \widetilde{s})$ and in $(\widetilde{s}, \frac{1}{2})$, respectively.

Proof. *Case (i).* We proceed by contradiction. Assume that there exists $s_a \in (0, \frac{1}{2})$ such that $\dot\lambda_1(s_a) = 0$. Then, recalling that $w_1 = w_1(x; s_a)$ does not vanish in $(0,1)$ by Proposition 3.3, by (32) we have

$$w_1'(s_a^+) + w_1'(s_a^-) = 0. \tag{53}$$

By (16) and (53), we have

$$b(s_a) w_1'(s_a^+) = -\lambda_1(s_a) \frac{m}{2} w_1(s_a), \tag{54}$$

$$b(s_a) w_1'(s_a^-) = \lambda_1(s_a) \frac{m}{2} w_1(s_a), \tag{55}$$

where $w_1(s_a) = w_1(x = s_a; s_a)$. Then, the restriction $w_1|_{(0,s_a)}, w_1|_{(s_a,1)}$ of the function w_1 to the sub-intervals $(0, s_a)$ and $(s_a, 1)$, respectively, – which will be denoted by the same symbol w_1 in the sequel – satisfies separately the two problems

$$\begin{cases}(bw_1')' + \lambda_1(s_a) b w_1 = 0, \quad x \in (0, s_a), & (56)\\ w_1(0) = 0, & (57)\\ b(s_a) w_1'(s_a) = \lambda_1(s_a) \dfrac{m}{2} w_1(s_a), & (58)\end{cases}$$

$$\begin{cases}(bw_1')' + \lambda_1(s_a) b w_1 = 0, \quad x \in (s_a, 1), & (59)\\ w_1(1) = 0, & (60)\\ b(s_a) w_1'(s_a) = -\lambda_1(s_a) \dfrac{m}{2} w_1(s_a), & (61)\end{cases}$$

Note that condition (15) (e.g., $[[w(s_a)]] = 0$) can always be satisfied by an appropriate scaling of $w_1|_{(0,s_a)}$ and $w_1|_{(s_a,1)}$. By changing variables $z(x) = 1 - x$ in (59)–(61), by the symmetry of b and using (49), the problem (59)–(61) can be written as

$$\begin{cases}(b\hat{w}_1')' + \lambda_1(s_a) b \hat{w}_1 = 0, \quad x \in (0, 1 - s_a), & (62)\\ \hat{w}_1(0) = 0, & (63)\\ b(1 - s_a) \hat{w}_1'(1 - s_a) = \lambda_1(s_a) \dfrac{m}{2} \hat{w}_1(1 - s_a), & (64)\end{cases}$$

where $\hat{w}(z(x)) = w(1 - z(x))$. More generally, let us denote by $\{\eta_n\}_{n \geqslant 1}$ the eigenvalues of the problem

$$\begin{cases}(bu')' + \eta b u = 0, \quad x \in (0, s_a), & (65)\\ u(0) = 0, & (66)\\ b(s_a) u'(s_a) = \eta \dfrac{m}{2} u(s_a), & (67)\end{cases}$$

and by $\{\mu_k\}_{k \geqslant 1}$ those of the problem (written with respect to the independent variable x)

$$\begin{cases}(bv')' + \mu b v = 0, \quad x \in (0, 1 - s_a), & (68)\\ v(0) = 0, & (69)\\ b(1 - s_a) v'(1 - s_a) = \mu \dfrac{m}{2} v(1 - s_a). & (70)\end{cases}$$

From the physical point of view, the eigenvalue problem (65)–(67) (respectively, (68)–(70)) corresponds to the free vibration of a cantilever $b = b(x)$ with end at $x = 0$ clamped and carrying a point mass $\frac{m}{2}$ at the other end $x = s_a$ (respectively, $x = 1 - s_a$). The function $w_1|_{(0,s_a)}$ is the first eigenfunction of (65)–(67) and it corresponds to the eigenvalue $\eta_1 = \lambda_1(s_a)$ by construction. This follows from the fact that $w_1|_{(0,s_a)}$ does not vanish in $(0, s_a]$ (by Proposition 3.3) and that the first eigenfunction of (65)–(67) has no zeros in $(0, s_a]$. This last property can be proved by using the same arguments of the proof of Proposition 3.3. Similarly, the function $w_1|_{(0,1-s_a)}$ (after the change of variables $z(x) = 1 - x$) is the first eigenfunction of (68)–(70) with $\mu_1 = \lambda_1(s_a)$.

We shall prove that if $s_a \in (0, \frac{1}{2})$, then $\mu_1 < \eta_1$, a contradiction.

By the variational formulation of the eigenvalue problem (68)–(70), we have

$$\mu_1 = \min_{\psi \in H^1_{(0)}(0,1-s_a) \setminus \{0\}} \frac{\int_0^{1-s_a} b(\psi')^2}{\int_0^{1-s_a} b\psi^2 + \frac{m}{2}\psi^2(1 - s_a)}, \tag{71}$$

where $H^1_{(0)}(0, 1 - s_a) = \{f : (0, 1 - s_a) \to \mathbb{R} \mid \int_0^{1-s_a} (f^2 + (f')^2) < \infty, f(0) = 0\}$. We select in (71) a restricted class of test functions belonging to $H^1_{(0)}(0, 1 - s_a)$ by taking

$$\psi(x) = \begin{cases} \varphi(x), & x \in (0, s_a),\\ \varphi(s_a), & x \in (s_a, 1 - s_a),\end{cases} \tag{72}$$

where $\varphi \in H^1_{(0)}(0, s_a)$. Then, the minimum in (71) cannot decrease, and we have

$$\mu_1 \leqslant \min_{\varphi \in H^1_{(0)}(0,s_a) \setminus \{0\}} \frac{\int_0^{s_a} b(\varphi')^2}{\int_0^{s_a} b\varphi^2 + \varphi^2(s_a) \int_{s_a}^{1-s_a} b + \frac{m}{2}\varphi^2(s_a)}. \tag{73}$$

In (73) we choose φ coincident with the eigenfunction associated to the first eigenvalue of the problem (65)–(67), say $\varphi = u_{1\eta}$. Again, the minimum cannot decrease and we have

$$\mu_1 \leqslant \frac{\int_0^{s_a} b(u_{1\eta}')^2}{\int_0^{s_a} b u_{1\eta}^2 + u_{1\eta}^2(s_a) \int_{s_a}^{1-s_a} b + \frac{m}{2} u_{1\eta}^2(s_a)}. \tag{74}$$

Since $s_a \in (0, \frac{1}{2})$, we have $\int_{s_a}^{1-s_a} b > 0$. Moreover, it is known that $u_{1\eta}^2(s_a) \neq 0$. Then

$$\mu_1 < \frac{\int_0^{s_a} b(u_{1\eta}')^2}{\int_0^{s_a} b u_{1\eta}^2 + \frac{m}{2} u_{1\eta}^2(s_a)} = \eta_1, \tag{75}$$

which is the desired contradiction. We have proved that the first derivative of $\lambda_1 = \lambda_1(s)$ never vanishes in $(0, \frac{1}{2})$. Since, by Proposition 3.4, $0 < \lambda_1(s) \leqslant \lambda_1^U$ in $[0, 1]$ and, by Proposition 5.1 (points (i) and (ii)), $\lambda_1(0) = \lambda_1^U$ and $\lambda_1(\frac{1}{2}) < \lambda_1^U$, the function $\lambda_1 = \lambda_1(s)$ is monotonically decreasing in $(0, \frac{1}{2})$.

Case (ii). By Proposition 3.4, we have $\lambda_2 \leqslant \lambda_2^U$ in $[0, 1]$ and, by Proposition 5.1 (points (i) and (ii)), $\lambda_2(0) = \lambda_2(\frac{1}{2}) = \lambda_2^U$. Then, there exists $\widetilde{s} \in (0, \frac{1}{2})$ such that $\dot{\lambda}_2(\widetilde{s}) = 0$. We need to prove the uniqueness of $\widetilde{s}$, that is, if $s_a \in (0, \frac{1}{2})$ and $s_b \in (0, \frac{1}{2})$ are such that $\dot{\lambda}_2(s_a) = \dot{\lambda}_2(s_b) = 0$, then we must have $s_a = s_b$.

As in Case (i), we proceed by contradiction, and we show that if $s_a \in (0, \frac{1}{2}), s_b \in (0, \frac{1}{2})$ are such that $\dot{\lambda}_2(s_a) = \dot{\lambda}_2(s_b) = 0$ with $s_a \neq s_b$, then we have a contradiction.

Without loss of generality we can assume $s_a < s_b$. Let us denote by $w_2 = w_2(x; s_a)$ the second eigenfunction of the fixed–fixed rod $b = b(x)$ (associated to the eigenvalue $\lambda_2(s_a)$) with a point mass m located at s_a.

We note that, by (32), if $\dot{\lambda}_2(s_a) = 0$, then $w_2'(s_a^+) + w_2'(s_a^-) = 0$. In fact, if $w_2(s_a) = 0$, then, by Proposition 5.1 (point (iv)) the unperturbed eigenfunction w_2^U vanishes at $x = s_a$. This contradicts the fact that, by symmetry, w_2^U vanishes at $x = \frac{1}{2}$ only.

By proceeding as it was made in Case (i) and taking into account the symmetry of b, it turns out that $(\lambda_2(s_a), w_2(x; s_a)|_{(0,s_a)})$ is an eigenpair of the eigenvalue problem

$$\begin{cases}(bw_2')' + \lambda_2(s_a) b w_2 = 0, \quad x \in (0, s_a), & (76)\\ w_2(0) = 0, & (77)\\ b(s_a) w_2'(s_a) = \lambda_2(s_a) \dfrac{m}{2} w_2(s_a), & (78)\end{cases}$$

and $(\lambda_2(s_a), w_2(x; 1 - s_a)|_{(0,1-s_a)})$ is an eigenpair of the eigenvalue problem (after changing variables $z(x) = 1 - x$)

$$\begin{cases}(bw_2')' + \lambda_2(s_a) b w_2 = 0, \quad x \in (0, 1 - s_a), & (79)\\ w_2(0) = 0, & (80)\\ b(1 - s_a) w_2'(1 - s_a) = \lambda_2(s_a) \dfrac{m}{2} w_2(1 - s_a). & (81)\end{cases}$$

Note that, in order to simplify the notation, in (78), expressions $w_2(s_a), w_2'(s_a)$ mean $w_2(x = s_a; s_a)$, $w_2'(x = s_a; s_a)$, respectively, and similarly in (81). Moreover, after changing variables $z(x) = 1 - x$, in problem (79)–(81), with a slight abuse of notation, we have denoted by the same symbol w_2 the function $\hat{w}_2(z(x)) = w_2(1 - z(x))$.

Similarly, suppose that $\dot{\lambda}_2(s_b) = 0$. Then, $w_2'(s_b^+) + w_2'(s_b^-) = 0$ and $(\lambda_2(s_b), w_2(x; s_b)|_{(0,s_b)} \equiv \widetilde{w}_2)$ is an eigenpair of the problem

$$\begin{cases}(b\widetilde{w}_2')' + \lambda_2(s_b) b \widetilde{w}_2 = 0, \quad x \in (0, s_b), & (82)\\ \widetilde{w}_2(0) = 0, & (83)\\ b(s_b) \widetilde{w}_2'(s_b) = \lambda_2(s_b) \dfrac{m}{2} \widetilde{w}_2(s_b), & (84)\end{cases}$$

and $(\lambda_2(s_b), w_2(x;1-s_b)|_{(0,1-s_b)} \equiv \widetilde{w}_2)$ is an eigenpair of the problem

$$\begin{cases} (b\widetilde{w}_2')' + \lambda_2(s_b) b\widetilde{w}_2 = 0, \quad x \in (0, 1-s_b), & (85)\\ \widetilde{w}_2(0) = 0, & (86)\\ b(1-s_b)\widetilde{w}_2'(1-s_b) = \lambda_2(s_b)\dfrac{m}{2}\widetilde{w}_2(1-s_b). & (87) \end{cases}$$

By Proposition 3.3, the 2nd vibrating mode $w_2 = w_2(x;s_a)$ has exactly one zero in $(0,1)$, say $x_2^{(1)}$, with $s_a < x_2^{(1)} < \frac{1}{2}$ by Proposition 10.5 in Appendix (Section A.3). Analogously, $\widetilde{w}_2 = w_2(x;s_b)$ vanishes in $(0,1)$ only at $\widetilde{x}_2^{(1)}$, with $s_b < \widetilde{x}_2^{(1)} < \frac{1}{2}$. By counting the number of zeros in the intervals $(0,s_a), (0,1-s_a), (0,s_b), (0,1-s_b)$ of the functions $w_2(x;s_a)|_{(0,s_a)}, w_2(x;1-s_a)|_{(0,1-s_a)}$, $w_2(x;s_b)|_{(0,s_b)}$, $w_2(x;1-s_b)|_{(0,1-s_b)}$, respectively, we can conclude that:

$w_2(x;s_a)|_{(0,s_a)}$ is the first eigenfunction of the eigenvalue problem (76)–(78), namely

$$\begin{cases} (bu')' + \eta bu = 0, \quad x \in (0, s_a), & (88)\\ u(0) = 0, & (89)\\ b(s_a)u'(s_a) = \eta\dfrac{m}{2}u(s_a) \quad \text{(eigenvalues } \{\eta_k\}_{k\geqslant 1}\text{)}; & (90) \end{cases}$$

$w_2(x;1-s_a)|_{(0,1-s_a)}$ is the second eigenfunction of the eigenvalue problem (79)–(81), namely

$$\begin{cases} (bu')' + \mu bu = 0, \quad x \in (0, 1-s_a), & (91)\\ u(0) = 0, & (92)\\ b(1-s_a)u'(1-s_a) = \mu\dfrac{m}{2}u(1-s_a) \quad \text{(eigenvalues } \{\mu_k\}_{k\geqslant 1}\text{)}; & (93) \end{cases}$$

$\widetilde{w}_2(x;s_b)|_{(0,s_b)}$ is the first eigenfunction of the eigenvalue problem (82)–(84), namely

$$\begin{cases} (bu')' + \kappa bu = 0, \ x \in (0, s_b), & (94)\\ u(0) = 0, & (95)\\ b(s_b)u'(s_b) = \kappa\dfrac{m}{2}u(s_b) \quad \text{(eigenvalues } \{\kappa_j\}_{j\geqslant 1}\text{)}; & (96) \end{cases}$$

and $\widetilde{w}_2(x;1-s_b)|_{(0,1-s_b)}$ is the second eigenfunction of the eigenvalue problem (85)–(87), namely

$$\begin{cases} (bu')' + \chi bu = 0, \quad x \in (0, 1-s_b), & (97)\\ u(0) = 0, & (98)\\ b(1-s_b)u'(1-s_b) = \chi\dfrac{m}{2}u(1-s_b) \quad \text{(eigenvalues } \{\chi_j\}_{j\geqslant 1}\text{)}. & (99) \end{cases}$$

By assumption, we have

$$\eta_1 = \mu_2, \quad \kappa_1 = \chi_2. \tag{100}$$

Then, to obtain the thesis, it is enough to show that the following strict inequalities hold

$$\kappa_1 < \eta_1, \tag{101}$$

$$\mu_2 < \chi_2. \tag{102}$$

In fact, by (100) and (101), (102), we have

$$\chi_2 = \kappa_1 < \eta_1 = \mu_2 < \chi_2, \tag{103}$$

that is $\chi_2 < \chi_2$, a contradiction.

The proof of (101) follows the same lines of the proof of (75). More precisely, by the variational formulation we have

$$\kappa_1 = \min_{\psi \in H^1_{(0)}(0,s_b)\setminus\{0\}} \frac{\int_0^{s_b} b(\psi')^2}{\int_0^{s_b} b\psi^2 + \frac{m}{2}\psi^2(s_b)}. \tag{104}$$

We restrict the set of test functions by assuming

$$\psi(x) = \begin{cases} \varphi(x), & x \in (0, s_a),\\ \varphi(s_a), & x \in (s_a, s_b), \end{cases} \tag{105}$$

with $\varphi \in H^1_{(0)}(0,s_a)$ (recall that $0 < s_a < s_b < \frac{1}{2}$). Then, the minimum cannot decrease:

$$\kappa_1 \leqslant \min_{\varphi \in H^1_{(0)}(0,s_a)\setminus\{0\}} \frac{\int_0^{s_a} b(\varphi')^2}{\int_0^{s_a} b\varphi^2 + \varphi^2(s_a)\int_{s_a}^{s_b} b + \frac{m}{2}\varphi^2(s_a)}. \tag{106}$$

Taking $\varphi = u_{1\eta}$ (that is, the first eigenfunction of (88)–(90) associated to the eigenvalue η_1) the minimum cannot decrease and we have

$$\kappa_1 \leqslant \frac{\int_0^{s_a} b(u_{1\eta}')^2}{\int_0^{s_a} bu_{1\eta}^2 + u_{1\eta}^2(s_a)\int_{s_a}^{s_b} b + \frac{m}{2}u_{1\eta}^2(s_a)}. \tag{107}$$

Since $u_{1\eta}^2(s_a) \neq 0$ and $\int_{s_a}^{s_b} b > 0$ (recall that $s_a < s_b$), and using the definition of the Rayleigh's Quotient we have

$$\kappa_1 < \frac{\int_0^{s_a} b(u_{1\eta}')^2}{\int_0^{s_a} bu_{1\eta}^2 + \frac{m}{2}u_{1\eta}^2(s_a)} = R[u_{1\eta}] = \eta_1, \tag{108}$$

which is (101).

The proof of (102) makes use of the Maximum–Minimum characterization of the eigenvalues (28). We have

$$\mu_2 = \min_{\psi \in H^1_{(0)}(0,1-s_a)\setminus\{0\},\ l_1^*(\psi)=0} \frac{\int_0^{1-s_a} b(\psi')^2}{\int_0^{1-s_a} b\psi^2 + \frac{m}{2}\psi^2(1-s_a)}, \tag{109}$$

where

$$l_1^*(\psi) = \int_0^{1-s_a} b\psi u_{1\eta} + \frac{m}{2}\psi(1-s_a)u_{1\eta}(1-s_a), \tag{110}$$

and $u_{1\mu}$ is the first eigenfunction of (91)–(93). We restrict the set of the test functions by taking

$$\psi(x) = \begin{cases} \varphi(x), & x \in (0, 1-s_b),\\ \varphi(1-s_b), & x \in (1-s_b, 1-s_a), \end{cases} \tag{111}$$

where $\varphi \in H^1_{(0)}(0, 1-s_b)$ (recall that $0 < s_a < s_b < \frac{1}{2}$). Then, the minimum cannot decrease and we have

$$\mu_2 \leqslant \min_{\varphi \in H^1_{(0)}(0,1-s_b)\setminus\{0\},\ l_1^*(\varphi)=0} \frac{\int_0^{1-s_b} b(\varphi')^2}{\int_0^{1-s_b} b\varphi^2 + \varphi^2(1-s_b)\int_{s_a}^{s_b} b + \frac{m}{2}\varphi^2(1-s_b)}, \tag{112}$$

where

$$l_1^*(\varphi) = \int_0^{1-s_b} b\varphi u_{1\eta} + \varphi(1-s_b)\int_{1-s_b}^{1-s_a} bu_{1\mu} + \frac{m}{2}\varphi(1-s_b)u_{1\eta}(1-s_a). \tag{113}$$

Now, we evaluate the minimum of the Rayleigh's Quotient shown in (112) under a generic constraint $\widetilde{l}_1(\varphi) = 0$, where $\widetilde{l}_1$ is a linear continuous functional on $H^1_{(0)}(0, 1-s_b)$, and we take the maximum on all the possible choices of $\widetilde{l}_1 \in (H^1_{(0)}(0, 1-s_b))'$. Then, the minimum in (112) cannot decrease, and we have

$$\mu_2 \leqslant \max_{\widetilde{l}_1 \in (H^1_{(0)}(0,1-s_b))'} \min_{\varphi \in H^1_{(0)}(0,1-s_b)\setminus\{0\},\ \widetilde{l}_1^*(\varphi)=0} \frac{\int_0^{1-s_b} b(\varphi')^2}{\int_0^{1-s_b} b\varphi^2 + \varphi^2(1-s_b)\int_{s_a}^{s_b} b + \frac{m}{2}\varphi^2(1-s_b)}. \tag{114}$$

By the Maximum–Minimum Principle, the right hand side of (115) is the second eigenvalue, say $\widetilde{\chi}_2$, of the following problem

$$\begin{cases} (bu')' + \widetilde{\chi} bu = 0, \quad x \in (0, 1 - s_b), & (115) \\ u(0) = 0, & (116) \\ b(1 - s_b)u'(1 - s_b) = \widetilde{\chi}\left(\frac{m}{2} + \int_{s_a}^{s_b} b\right) u(1 - s_b). & (117) \end{cases}$$

Note that problem (115)–(117) describes the free longitudinal vibration of a cantilever rod with a point mass of intensity $\left(\frac{m}{2} + \int_{s_a}^{s_b} b\right)$ at the right end. Since $\int_{s_a}^{s_b} b > 0$ and every eigenfunction of (115)–(117) does not vanish at $x = 1 - s_b$, by Monotonicity theorems we have

$$\widetilde{\chi}_2 < \chi_2, \tag{118}$$

which implies $\mu_2 < \chi_2$, and the proof of the inequality (102) is complete. □

6. A λ-curves based identification algorithm

In this section we prove Theorem 2.3. The proof is constructive and leads to an algorithm for the determination of the parameters $\{s, m\}$ in the problem (14)–(17) from the knowledge of the first two natural frequencies. Let $\{\overline{\lambda}_1, \overline{\lambda}_2\}$ be the experimental values of the first two eigenvalues of (14)–(17), for a given, strictly positive $b, b \in C^1([0,1])$ and $b(x) = b(1-x)$ in $[0,1]$, and for certain $s \in (0,1), 0 < m < \infty$. The input data are assumed to satisfy conditions (31), precisely

$$0 < \overline{\lambda}_1 < \lambda_1^U, \quad \lambda_1^U \leqslant \overline{\lambda}_2 \leqslant \lambda_2^U. \tag{119}$$

Note that, by Propositions 5.1 and 3.3, the upper bound in the left inequality of (119) is strict, that is the first eigenvalue is always "sensitive" to the presence of the point mass m when $s \in (0,1)$.

If $\overline{\lambda}_2 = \lambda_2^U$, then by Propositions 5.1 and 5.3 the point mass m is located at $s = \frac{1}{2}$. By Proposition 5.1, $\lambda_1 = \lambda_1\left(\frac{1}{2}, m\right)$ is a monotonically decreasing function of m and, in addition,

$$\lim_{m \to \infty} \lambda_1\left(\frac{1}{2}, m\right) = 0^+. \tag{120}$$

The simpler way to prove (120) is to come back to the original crack-problem (9)–(12) and take the limit of the first (positive) eigenvalue as $K \to 0^+$. Roughly speaking, when $K \to 0^+$, the rod splits in two rods of length s and $1 - s$, both under free–free end conditions. Clearly, $\lambda_1(K) \to 0^+$ as $K \to 0^+$. By (120) and by the monotonicity of the function $\lambda_1\left(\frac{1}{2}, \cdot\right)$ for $m \in [0, \infty)$, we can uniquely determine m by solving $\overline{\lambda}_1 = \lambda_1\left(\frac{1}{2}, m\right)$.

In the remaining of the section we shall consider the nontrivial condition $\overline{\lambda}_2 < \lambda_2^U$ and, by symmetry (see Proposition 5.3), we assume $s \in \left(0, \frac{1}{2}\right)$.

The main steps of the algorithm are presented in the sequel.

We start by determining the values $m_1^-, m_2^-, 0 < m_i^- < \infty$, $i = 1, 2$, of the parameter m such that

$$\overline{\lambda}_1 = \lambda_1\left(\frac{1}{2}, m_1^-\right), \tag{121}$$

$$\overline{\lambda}_2 = \lambda_2\left(s_{2min}, m_2^-\right), \tag{122}$$

where (by Theorem 5.5, part ii) $s_{2min} \in \left(0, \frac{1}{2}\right)$ is the unique point such that $\frac{\partial \lambda_2}{\partial s}(s_{2min}, m_2^-) = 0$. Note that $m_1^- \neq m_2^-$ and, clearly, m_1^-, m_2^- are estimates from below of the unknown parameter m:

$$m_2^- \leqslant m, \qquad m_1^- < m. \tag{123}$$

We consider preliminarily the special case in which the curve $y = \lambda_1(s, m_2^-)$ and the straight line $y = \overline{\lambda}_1$ have a (unique) intersection point P with abscissa coinciding with s_{2min}. In this case, obviously, we have $m = m_2^-$ and $s = s_{2min}$. If the above condition is not satisfied, e.g., if either the intersection point does not exist or its abscissa is different from s_{2min}, then

$$\max\{m_1^-, m_2^-\} < m \tag{124}$$

and we need to distinguish two main cases.

First Case:

$$\max\{m_1^-, m_2^-\} = m_1^-. \tag{125}$$

In a reference cartesian system (y, s), we determine the curve $y = \lambda_2(s, m_1^-)$ (see the dashed curve in Fig. 2). By Proposition 5.1 and Theorem 5.5 (point ii), the curve $y = \lambda_2(s, m_1^-)$ intersects the straight line $y = \overline{\lambda}_2$ exactly at two points, say $P_{2l}^{(1)}, P_{2r}^{(1)}$, located to the left $(P_{2l}^{(1)})$ and to the right $(P_{2r}^{(1)})$ of the point $P_{2min} = (s_{2min}, \overline{\lambda}_2)$. Let us denote by $s_{2l}^{(1)}, s_{2r}^{(1)}$ their abscissa, respectively. The curve $y = \lambda_1(s, m_1^-)$ is tangent at $P_1^{(1)} = \left(s_1^{(1)} = \frac{1}{2}, \overline{\lambda}_1\right)$ to the straight line $y = \overline{\lambda}_1$.

Suppose to increase continuously m from m_1^- to, say, $m^* > m_1^-$, with m^* not too large. We obtain two curves $y = \lambda_2(s, m^*), y = \lambda_1(s, m^*)$ (see the dotted curves in Fig. 2). The abscissa of the intersection points $P_{2l}^{(2)}, P_{2r}^{(2)}$ between $y = \lambda_2(s, m^*)$ and $y = \overline{\lambda}_2$ are $s_{2l}^{(2)}, s_{2r}^{(2)}$, respectively. The point $P_{2r}^{(2)}$ moves to the right of $P_{2r}^{(1)}$, and $P_{2l}^{(2)}$ to the left of $P_{2l}^{(1)}$. The abscissa of the intersection point $P_1^{(2)}$ between $y = \lambda_1(s, m^*)$ and $y = \overline{\lambda}_1$ is $s_1^{(2)}$, and $P_1^{(2)}$ moves to the left of $P_1^{(1)}$. (Note that, since $s_{2r}^{(1)} < s_1^{(1)} = \frac{1}{2}$, by continuity, such a choice of m^* is always possible.) It follows that, for $m^* > m_1^-$ and m^* not too large, $s_{2r}^{(2)}$ and $s_1^{(2)}$ (with $s_{2r}^{(2)} < s_1^{(2)}$) move one toward each other. By increasing continuously m (from m_1^- to ∞, say), the intersection point P_1 between $y = \lambda_1(s, m)$ and the straight line $y = \overline{\lambda}_1$ moves from the right to the left, its abscissa $s_1 = s(P_1)$ is a monotonically decreasing function of m and, moreover, $\lim_{m \to \infty} s(P_1) = 0^+$. (Note that if $s(P_1)$ has an accumulation point at $s_\infty > 0$ as $m \to \infty$, then we can find a contradiction with

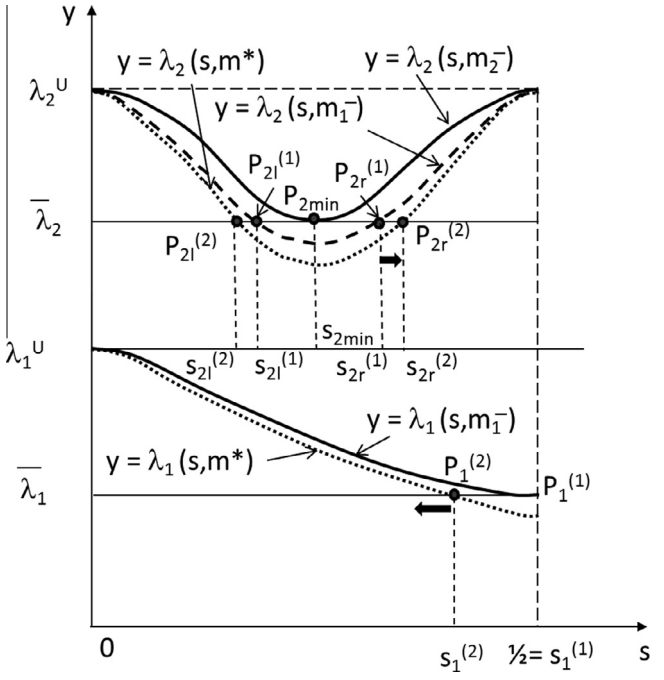

Fig. 2. A λ–curves damage identification algorithm based on resonant frequency data: first case.

Proposition 5.1.) Simultaneously, the point P_{2r} obtained as the right intersection of $y = \lambda_2(s,m)$ and $y = \overline{\lambda}_2$ is such that $s_{2r} = s(P_{2r})$ is monotonically increasing as m increases. Then, we can conclude that there exists a unique value $\widetilde{m}$ such that $s_{2r} = s_1$. The value $\widetilde{m}$ is the intensity of the mass, and $s = s_1$ is its position.

Second Case:

$$\max\{m_1^-, m_2^-\} = m_2^-. \tag{126}$$

In this case, we determine the curve $y = \lambda_1(s, m_2^-)$. This curve has only one point of intersection with the straight line $y = \overline{\lambda}_1$, say $P_1^{(1)}$, with abscissa $s_1^{(1)} = s(P_1^{(1)})$ such that $0 < s_1^{(1)} < \frac{1}{2}$. Here, we need to distinguish two subcases, indicated by (a) and (b) in what follows, depending on the relative position of s_{2min} and $s_1^{(1)}$.

Second Case – (a):

$$s_{2min} \leqslant s_1^{(1)}. \tag{127}$$

The situation is illustrated in Fig. 3. If $s_{2min} = s_1^{(1)}$, then the inverse problem is solved. If $s_{2min} < s_1^{(1)}$, then we can repeat the procedure used in the First Case. In brief, by increasing continuously m, with $m > m_2^-$, the points P_1 (intersection between $y = \lambda_1(s,m)$ and $y = \overline{\lambda}_1$) and P_{2r} (right intersection between $y = \lambda_2(s,m)$ and $y = \overline{\lambda}_2$) shown in Fig. 3 move toward each other. Since $\lim_{m\to\infty} s(P_1) = 0^+$ and $s(P_{2r})$ is increasing with respect to m, there exists exactly one value $\widetilde{m}$ such that $s(P_1) = s(P_{2r})$, and the problem is solved.

Second Case – (b):

$$s_{2min} > s_1^{(1)}. \tag{128}$$

In this case, by increasing m (from m_2^- to ∞), both the points P_{2l} (left intersection between $y = \lambda_2(s,m)$ and $y = \overline{\lambda}_2$) and $P_1^{(2)}$ (intersection between $y = \lambda_1(s,m)$ and $y = \overline{\lambda}_1$) move to the left, see Fig. 4, and we need to change our arguments. We use the following property: there exists m^*, $m^* > m_2^-$ and m^* large enough, such that the left intersection point P_{2l}^* between $y = \lambda_2(s,m^*)$ and $y = \overline{\lambda}_2$ is to the left of $P_1^{(1)}$, that is $s_2^* = s(P_{2l}^*) < s(P_1^{(1)})$, see Fig. 5. (In fact, one can prove that $\lim_{m\to\infty} s(P_2^*(m)) = 0^+$.) Now, by decreasing m (from m^* to m_2^-), the left intersection point $P_{2l}(m)$ between $y = \lambda_2(s,m)$ and $y = \overline{\lambda}_2$ moves monotonically to the right, and $\lim_{m\to m_2^-} s(P_{2l}(m)) = s_{2min}$, whereas, by increasing m (from m_2^- to ∞), the intersection point $P_1(m)$ between $y = \lambda_1(s,m)$ and $y = \overline{\lambda}_1$ moves monotonically to the left, and $\lim_{m\to\infty} s(P_1(m)) = 0^+$. Therefore, there exists a unique value of m, say $\widetilde{m}$, with $\widetilde{m} \in (m_2^-, m^*)$, such that $s(P_{2l}(\widetilde{m})) = s(P_1(\widetilde{m}))$, and the problem is solved.

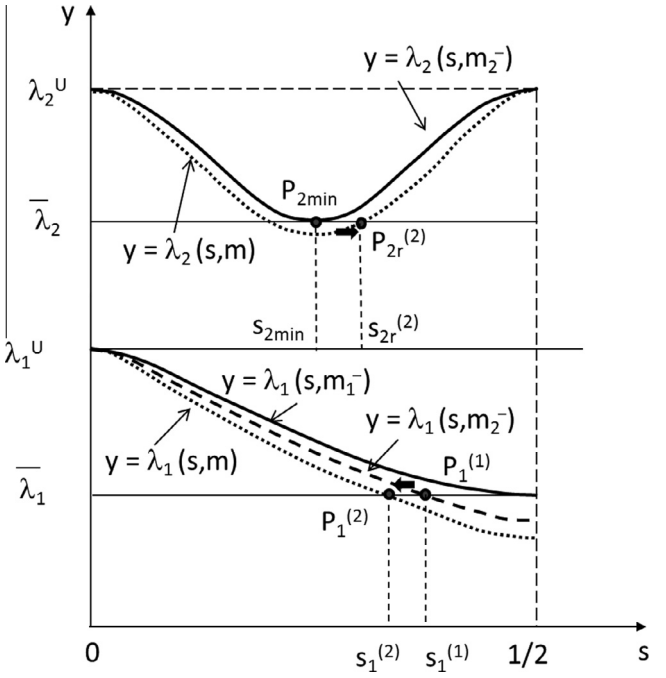

Fig. 3. A λ–curves damage identification algorithm based on resonant frequency data: second case, subcase (a).

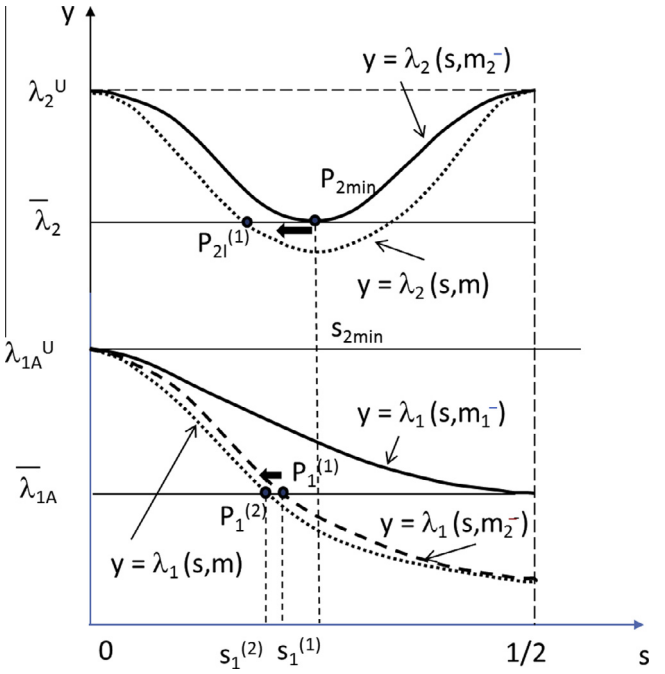

Fig. 4. A λ–curves damage identification algorithm based on resonant frequency data: second case, subcase (b).

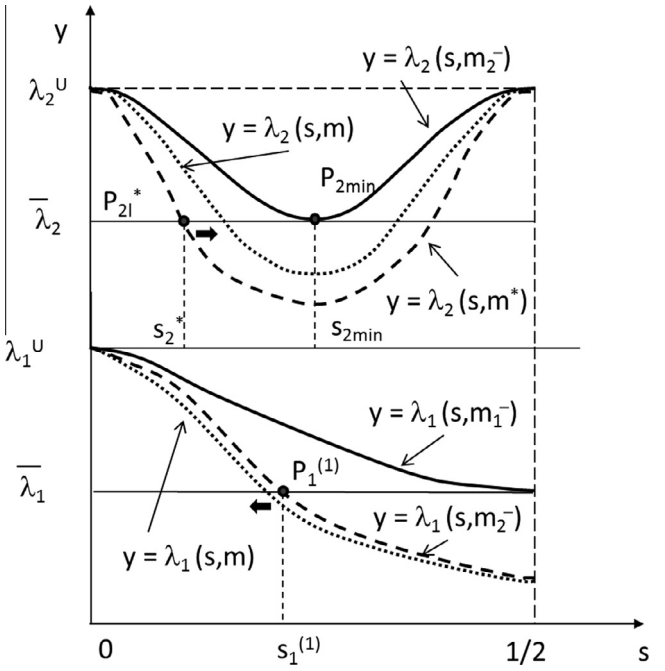

Fig. 5. A λ–curves damage identification algorithm based on resonant frequency data: new argument for second case, subcase (b).

In conclusion, we have presented a constructive algorithm for the unique identification of the position s and intensity m of the point mass (e.g., equivalently, the position s and the severeness $K = m^{-1}$ of the crack, see Proposition 2.1) from the knowledge of the first two eigenfrequencies of (14)–(17). As the referential rod is symmetric with respect to the mid-point, the position s of the point mass is determined up to the symmetric position $1 - s$. In the next section we shall show that the indeterminacy due to the symmetry can be removed by replacing the information on the second natural frequency by the knowledge of a suitable antiresonant frequency of the rod.

7. Identification by one resonant and one antiresonant frequency

In this section we shall prove that the crack in the rod (14)–(17) can be uniquely located using the first natural frequency of the cracked rod and the first antiresonant frequency of the driving point frequency response function (FRF) of the rod evaluated at one free end, say at $x = 0$. These antiresonances are the zeros of the FRF $H(\omega; 0, 0)$, and they coincide with the natural frequencies of the cracked rod when the longitudinal displacement at the cross-section $x = 0$ is hindered. Therefore, the antiresonances of $H(\omega; 0, 0)$ are the natural frequencies of the cantilever rod supported at $x = 0$. Under the same notation of Section 2, the corresponding eigenvalue problem written in dimensionless form is

$$\begin{cases} (au')' + \lambda au = 0, \quad x \in (0, s) \cup (s, 1), & (129)\\ u(0) = 0, & (130)\\ [[au'(s)]] = 0, & (131)\\ K[[u(s)]] = a(s)u'(s), & (132)\\ u'(1) = 0. & (133) \end{cases}$$

By adapting the proof of Proposition 2.1, it turns out that the eigenvalue problem (129)–(133) for the cracked supported-free rod is equivalent to the following eigenvalue problem for a free-supported rod with a point mass at $x = s$:

$$\begin{cases} (bw')' + \lambda bw = 0, \quad x \in (0, s) \cup (s, 1), & (134)\\ w'(0) = 0, & (135)\\ [[w(s)]] = 0, & (136)\\ [[bw'(s)]] = -\lambda m w(s), & (137)\\ w(1) = 0, & (138) \end{cases}$$

where, as in (18), $b = a^{-1}$ and $m = K^{-1}$, and the symmetry assumption $b(x) = b(1 - x)$ on b is maintained. We shall denote by

$$0 < \lambda_{1A} < \lambda_{2A} < \dots \tag{139}$$

the eigenvalues of (134)–(138).

The qualitative properties of the eigenvalue problem (134)–(138) useful for our treatment can be derived as it was done in Section 3 for the problem (14)–(17). The eigenvalue derivative expressions (32), (33) still hold in the present case, and eigenpair sensitivity properties can be deduced following the lines shown in the first part of Section 5. Most of the steps in the preceding proofs can be duplicated, with proper modifications, and will not repeated here. Instead, we shall consider in some detail the qualitative behavior of the λ-s curve for the first eigenvalue λ_{1A}, which is the key property used in the identification algorithm illustrated at the end of the present section.

The following result is the equivalent of point (ii) in Theorem 5.5.

Theorem 7.1. *Let (λ_{1A}, w_1) be the first eigenpair of (134)–(138) for b strictly positive, continuously differentiable function in $[0, 1]$. Let m be given, $0 < m < \infty$. Then $\dot\lambda_{1A}(0) > 0, \dot\lambda_{1A}(1) = 0$, and $\lambda_{1A} = \lambda_{1A}(s)$ is a strictly increasing function in $(0, 1)$.*

Proof. By (32), we have $\dot\lambda_{1A}(1) = 0$. Observing that $\dot\lambda_{1A}(0) = -\lambda_{1A}\frac{m w_1(0) w_1'(0)}{m w_1^2(0) + \int_0^1 b w_1^2}$ and recalling that, for a mass m placed at $x = 0$ the end condition is $b(0)w_1'(0) = -\lambda_{1A} m w_1(0)$, we easily get $\dot\lambda_{1A}(0) = \frac{\lambda_{1A}^2 m^2 w_1^2(0)}{b(0)\left(m w_1^2(0) + \int_0^1 b w_1^2\right)}$. Since $w_1(0) \neq 0$, the above expression implies $\dot\lambda_{1A}(0) > 0$.

In order to prove that $\lambda_{1A} = \lambda_{1A}(s)$ is a monotonically increasing function of s, it is enough to prove that $\dot\lambda_{1A}$ never vanishes in $(0, 1)$. Note that $\lambda_{1A}(s) \leqslant \lambda_{1A}^U$ and that $\lambda_{1A}(0) < \lambda_{1A}^U$, where λ_{1A}^U is the unperturbed antiresonance value, e.g., the first eigenvalue of the problem (134)–(138) for $m = 0$.

We proceed by contradiction. Assume that there exists $s_a \in (0, 1)$ such that $\dot\lambda_{1A}(s_a) = 0$. Then, by (32), we have

$$w_1'(s_a^+) + w_1'(s_a^-) = 0. \tag{140}$$

By (140) and (136), (137) we have

$$b(s_a) w_1'(s_a^+) = -\lambda_{1A}(s_a)\frac{m}{2} w_1(s_a), \tag{141}$$

$$b(s_a) w_1'(s_a^-) = \lambda_{1A}(s_a)\frac{m}{2} w_1(s_a). \tag{142}$$

It follows that the restriction of the function $w_1 = w_1(x; s_a)$ (which is the eigenfunction associated to the first eigenvalue $\lambda_{1A}(s_a)$ of (134)–(138)) to the intervals $(0, s_a)$ and $(s_a, 1)$ satisfies separately the two eigenvalue problems

$$\begin{cases} (b w_1')' + \lambda_{1A}(s_a) b w_1 = 0, \quad x \in (0, s_a), & (143)\\ w_1'(0) = 0, & (144)\\ b(s_a) w_1'(s_a) = \lambda_{1A}(s_a)\frac{m}{2} w_1(s_a), & (145) \end{cases}$$

$$\begin{cases} (b w_1')' + \lambda_{1A}(s_a) b w_1 = 0, \quad x \in (s_a, 1), & (146)\\ w_1(1) = 0, & (147)\\ b(s_a) w_1'(s_a) = -\lambda_{1A}(s_a)\frac{m}{2} w_1(s_a), & (148) \end{cases}$$

The problem (143)–(145) describes the free vibration of a rod with free end at $x = 0$ and with a point mass m at the end $x = s$. We recall that the function w_1, as first eigenfunction of the problem (134)–(138), does not vanish in $[0, 1)$. Then, its restriction $w_1|_{(0,s_a)}$ to the subinterval $[0, s_a]$ does not vanish, and then $w_1|_{(0,s_a)}$ is the first eigenfunction of the eigenvalue problem (143)–(145). But the first eigenfunction of (143)–(145) is associated to the zero eigenvalue, that is $\lambda_{1A}(s_a) = 0$, which is a contradiction since the fundamental eigenvalue of (134)–(138) is strictly positive (see (139)). The proof of the theorem is complete. □

We conclude this section with the following reconstruction result: the measurement of the first natural frequency λ_1 of (14)–(17) and the first antiresonant frequency λ_{1A} of (134)–(138) allows for a unique determination of the position s of the point mass and of its intensity m.

To prove the above statement, it is enough to adapt the algorithm presented in Section 6. The main steps of the procedure are presented in the sequel. Note that, by the Variational Theory of eigenvalues, $\lambda_{1A}(s) < \lambda_1(s)$ in $[0, 1)$.

Let us denote by $\bar\lambda_1, \bar\lambda_{1A}$ the measured frequency data. As a first step, we determine the values m_1^-, m_{1A}^- such that

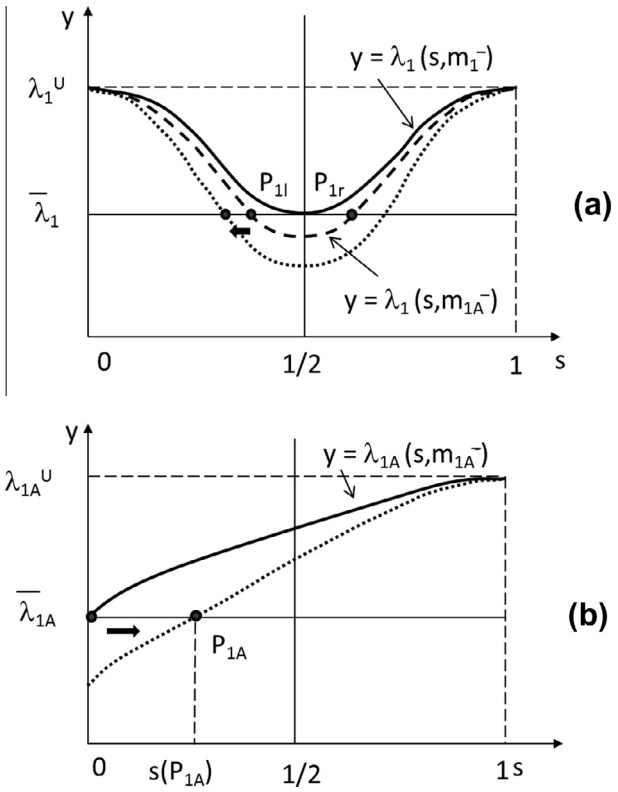

Fig. 6. A λ–curves damage identification algorithm based on resonant and antiresonant frequency data: first case.

$\lambda_1(\frac{1}{2}, m_1^-) = \overline{\lambda}_1, \lambda_{1A}(0, m_{1A}^-) = \overline{\lambda}_{1A}$. Clearly, $m_1^- \neq m_{1A}^-$ and $m > \max\{m_1^-, m_{1A}^-\}$.

Suppose that $m_{1A}^- > m_1^-$. Then, we can follow a procedure similar to that used in the First Case of the identification algorithm shown in Section 6, see Fig. 6. First, we determine the curve $y = \lambda_1(s, m_{1A}^-)$. The two points of intersection of this curve with the straight line $y = \overline{\lambda}_1$ are symmetrically placed with respect to $s = \frac{1}{2}$, say P_{1l} and P_{1r}. By increasing continuously m (from m_{1A}^- to ∞), the left point P_{1l} moves monotonically to the left of $s = \frac{1}{2}$, and $\lim_{m\to\infty} s(P_{1l}) = 0^+$. Simultaneously, the point P_{1A} given by the intersection of the curve $y = \lambda_{1A}(s, m)$ with the straight line $y = \overline{\lambda}_{1A}$ moves monotonically to the right of $s = 0$ for monotonically increasing values of m (from m_{1A}^- to ∞). Then, there exists a unique $\widetilde{s} \in (0, \frac{1}{2})$ such that $\widetilde{s} = s(P_{1A}) = s(P_{1l})$, and the problem is solved.

Assume now that $m_{1A}^- < m_1^-$. In this case, we determine the curve $y = \lambda_{1A}(s, m_1^-)$ and, as we did in Section 6 (Second Case), we need to distinguish two cases, case (a) and case (b), depending whether the abscissa $s(P_{1A})$ of the intersection point P_{1A} between $y = \lambda_{1A}(s, m_1^-)$ and $y = \overline{\lambda}_{1A}$ is greater or less than $\frac{1}{2}$. In brief, if $s(P_{1A}) \leqslant \frac{1}{2}$, then we can follow an argument similar to that employed above. Otherwise, if $s(P_{1A}) > \frac{1}{2}$, then we determine m^* large enough such that the intersection point P_{2r}^* between $y = \lambda_1(s, m^*)$ and $y = \overline{\lambda}_1$ is to the right of P_{1A}, that is $s(P_{2r}^*) > s(P_{1A})$, see Fig. 7. Finally, by decreasing monotonically m (from m^*) in the graph $y = \lambda_1(s, m)$ and increasing monotonically m (from m_1^-) in the graph $y = \lambda_{1A}(s, m)$, we can solve the identification problem.

8. Extensions

In this section we generalize the results obtained in Section 7 to (symmetric) rods whose vibrations are described by

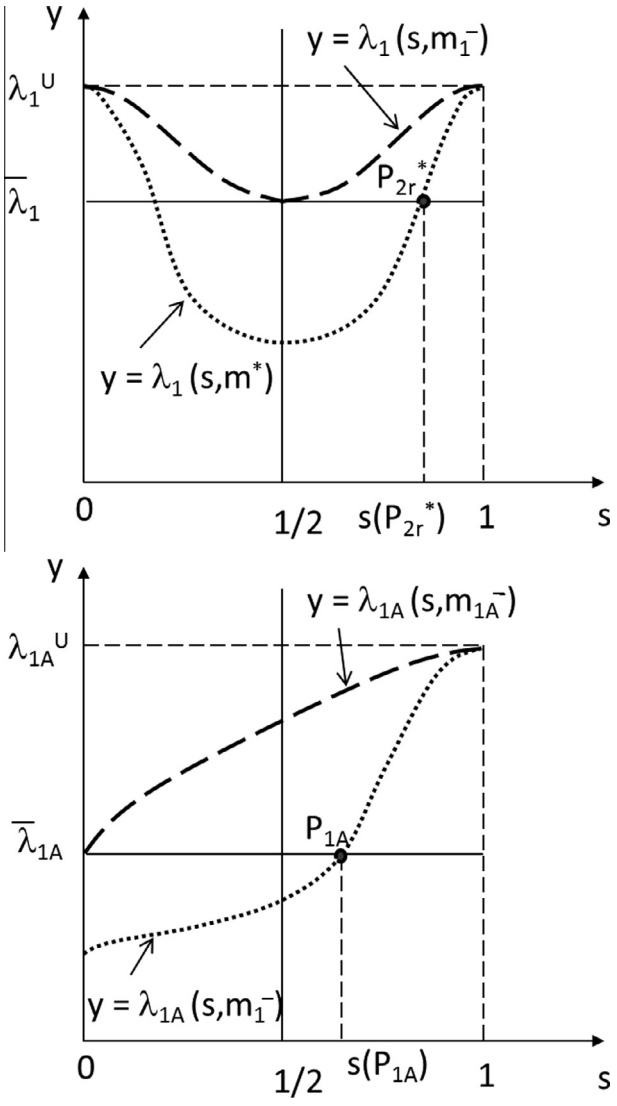

Fig. 7. A λ–curves damage identification algorithm based on resonant and antiresonant frequency data: second case.

Sturm–Liouville operators more general than those appearing in (9)–(12). As before, the identification method is based on the behavior of the λ–m and λ–s curves for the corresponding eigenvalue problems. In turn, these properties follow from qualitative results on the eigensolutions analogous to those presented in Section 3 and 4. Most of the steps in the preceding analysis can be repeated and, therefore, in the sequel we shall state the main results and we omit the details of the proofs.

Let us consider the cracked rod under free–free end conditions introduced at the beginning of Section 2, with a crack of severity K at the position $s \in (0, 1)$. Here, differently from what previously assumed in (9)–(12), the axial stiffness $a = a(x)$ is not necessarily proportional to the linear mass density $\rho = \rho(x)$ of the rod. Therefore, the free undamped vibrations are governed by the eigenvalue problem

$$\begin{cases} (au')' + \lambda\rho u = 0, \quad x \in (0,s) \cup (s,1), & (149)\\ [[au'(s)]] = 0, & (150)\\ K[[u(s)]] = a(s)u'(s), & (151)\\ a(0)u'(0) = 0 = a(1)u'(1), & (152) \end{cases}$$

The functions a and ρ are assumed to be strictly positive continuously differentiable functions, satisfying the symmetry condition $a(x) = a(1-x)$ and $\rho(x) = \rho(1-x)$ in $[0, 1]$.

The eigenpairs of (149)–(152) are denoted by $\{(\lambda_n, u_n)\}_{n=0}^{\infty}$, where $\lambda_0 = 0$ is the eigenvalue associated to a rigid body motion of the rod. By adapting the proof of Proposition 2.1, it can be seen that the positive eigenvalues of (149)–(152) coincide with the eigenvalues of a rod carrying a point mass $m = K^{-1}$ at $x = s$, under supported-supported end conditions:

$$\begin{cases} (bw')' + \lambda r w = 0, \quad x \in (0,s) \cup (s,1), & (153)\\ [[w(s)]] = 0, & (154)\\ [[bw'(s)]] = -\lambda m w(s), & (155)\\ w(0) = 0 = w(1), & (156) \end{cases}$$

with

$$w = au' \quad \text{in } (0,s) \cup (s,1), \quad b = \rho^{-1} \text{ and } r = a^{-1} \text{ in } [0,1]. \tag{157}$$

A direct inspection of the proofs presented in the previous sections shows that the qualitative properties stated in Proposition 3.1, Proposition 3.3 and Proposition 3.4 can be extended to cover the present case. Moreover, the eigenvalue derivative expressions (32), (33) derived in Proposition 4.1 are now replaced by

$$\frac{\partial \lambda}{\partial s} = -\lambda \, \frac{m w(s)(w'(s^+) + w'(s^-))}{m w^2(s) + \int_0^1 r w^2}, \tag{158}$$

$$\frac{\partial \lambda}{\partial m} = -\lambda \, \frac{w^2(s)}{m w^2(s) + \int_0^1 r w^2}, \tag{159}$$

where (λ, w) is an eigenpair of (153)–(156). The above properties are used to prove the following analogue of Theorem 5.5, restricted to the first eigenvalue λ_1 of (153)–(156). As usual, let us denote by λ_1^U the corresponding *unperturbed* eigenvalue, e.g., the first eigenvalue of (153)–(156) for $m = 0$.

Theorem 8.1. *Let $\lambda_1 = \lambda_1(s)$ be the first eigenvalue of (153)–(156) for a given point mass m, $0 < m < \infty$, placed at s. Then, $\lambda_1(0) = \lambda_1(1) = \lambda_1^U$, $\dot\lambda_1(0) = \dot\lambda_1(1) = 0$, and there exists a unique $\widetilde{s} \in (0,1)$ such that $\dot\lambda_1(\widetilde{s}) = 0$, that is the function $\lambda_1 = \lambda_1(s)$ is strictly monotone decreasing and strictly monotone increasing in $(0,\widetilde{s})$ and in $(\widetilde{s},1)$, respectively.*

In order to state the main result of this section, we need to introduce the antiresonant frequencies of the driving-point FRF $H(\omega;0,0)$ of the free–free cracked rod. Following the analysis of Section 7 and adapting the proof of Proposition 2.1, these antiresonances are the eigenvalues of the problem for a free-supported rod with a point mass $m = K^{-1}$ at $x = s$:

$$\begin{cases} (bw')' + \lambda r w = 0, \quad x \in (0,s) \cup (s,1), & (160)\\ w'(0) = 0, & (161)\\ [[w(s)]] = 0, & (162)\\ [[bw'(s)]] = -\lambda m w(s), & (163)\\ w(1) = 0, & (164) \end{cases}$$

Then, it is possible to prove the following result.

Theorem 8.2. *For a given $m, 0 < m < \infty$, the first eigenvalue $\lambda_{1A} = \lambda_{1A}(s)$ of (160)–(164) is a strictly increasing function of s in $[0,1)$, with $\lambda_{1A}(0) < \lambda_{1A}^U, \lambda_{1A}(1) = \lambda_{1A}^U$, $\dot\lambda_{1A}(1) = 0$.*

The main consequence of Theorem 8.1 and Theorem 8.2 is the following improvement of the identification result stated in Section 7: *The knowledge of the first eigenvalue of the supported-supported rod and the first eigenvalue of the free-supported rod allows to determine uniquely the mass location and intensity.*

The reconstruction algorithm follows the lines of that presented in Section 7.

9. Applications

9.1. Discrete approximation of the eigenvalue problem

The application of the crack identification method illustrated in previous sections requires the implementation of a numerical model for the determination of the eigenvalues of the vibrating rod. With the aim of illustrating the main numerical aspects, we shall consider in detail the weak formulation (24), the analysis of other boundary conditions (see Section 7) or more general operators (see Section 8) being similar. The weak formulation (24) consists in finding $w \in H_0^1(0,1) \setminus \{0\}$ such that

$$\int_0^1 bw'\varphi' = \lambda\left(\int_0^1 bw\varphi + mw(s)\varphi(s)\right), \quad \text{for every } \varphi \in H_0^1(0,1). \tag{165}$$

To find a discrete version of (165), we can work on the finite dimensional subspace $\mathcal{H}$ of the piecewise-linear continuous functions. In fact, $\mathcal{H}$ is dense in $H_0^1(0,1)$, that is, for every $f \in H_0^1(0,1)$ and for every $\epsilon > 0$, there exists $\widetilde{f} \in \mathcal{H}$ such that $\|f - \widetilde{f}\|_{H^1(0,1)} < \epsilon$. More precisely, let us consider the following approximation $\widetilde{w}$ of w in (165):

$$\widetilde{w}(x) = \sum_{i=1}^{N} \varphi_i(x)\widetilde{w}_i, \tag{166}$$

where $\widetilde{w} = (\widetilde{w}_1, \ldots, \widetilde{w}_N) \in \mathbb{R}^N$ and the test functions $\varphi_i = \varphi_i(x)$, $i = 1, \ldots, N$, are defined as follows

$$\varphi_i(x) = \begin{cases} 0, & x \in [0,1] \setminus (x_{i-1}, x_{i+1}),\\ \frac{x - x_{i-1}}{x_i - x_{i-1}}, & x \in (x_{i-1}, x_i),\\ 1 - \frac{x - x_i}{x_{i+1} - x_i}, & x \in (x_i, x_{i+1}). \end{cases} \tag{167}$$

The mesh $\{x_0 = 0 < x_1 < \ldots < x_N < x_{N+1} = 1\}$ is chosen such that the nodes x_i are equally spaced, e.g., $x_{i+1} - x_i = \Delta x = \frac{1}{N+1}$, for every $i = 0, \ldots, N$, and there exists an index $i_s \in \{1, \ldots, N\}$, such that $s = i_s \Delta x$. Replacing (167) in (165), the discrete version of the eigenvalue problem (165) consists in finding $(\widetilde{\lambda}, \widetilde{w}), \widetilde{w} \in \mathbb{R}^N \setminus \{0\}$, solution to

$$K\widetilde{w} = \widetilde{\lambda} M \widetilde{w}, \tag{168}$$

where K, M are the $N \times N$ real symmetric matrix of the stiffness and of the inertia of the system. In particular,

$$M_{i,j} = M_{i,j} + m\delta_{i,i_s}\delta_{i_s,j}, \quad i,j = 1, \ldots, N, \tag{169}$$

where $M_{i,j} = 0$ if $|i - j| > 1$ and

$$M_{i,i} = \int_{x_{i-1}}^{x_{i+1}} b(x)\varphi_i^2(x)dx, \quad i = 1, \ldots, N, \tag{170}$$

$$M_{i,i+1} = \int_{x_i}^{x_{i+1}} b(x)\varphi_i(x)\varphi_{i+1}(x)dx, \quad i = 1, \ldots, N-1, \tag{171}$$

$$M_{i-1,i} = \int_{x_{i-1}}^{x_i} b(x)\varphi_{i-1}(x)\varphi_i(x)dx, \quad i = 2, \ldots, N. \tag{172}$$

Moreover, $K_{i,j} = 0$ if $|i - j| > 1$ and

$$K_{i,i} = \left(\frac{1}{\Delta x}\right)^2 \int_{x_{i-1}}^{x_{i+1}} b(x)dx, \quad i = 1, \ldots, N, \tag{173}$$

$$K_{i,i+1} = -\left(\frac{1}{\Delta x}\right)^2 \int_{x_i}^{x_{i+1}} b(x)dx, \quad i = 1, \ldots, N-1, \tag{174}$$

$$K_{i-1,i} = -\left(\frac{1}{\Delta x}\right)^2 \int_{x_{i-1}}^{x_i} b(x)dx, \quad i = 2, \ldots, N. \tag{175}$$

9.2. Numerical implementation of the identification method

A numerical code has been developed for the practical application of the damage identification method. For the sake of simplicity, reference is made to damage identification in a free–free rod from two natural frequencies.

Essentially, the algorithm follows the steps presented in Section 6, except for a slight change in case 2b. Under the notation of Section 6 (case 2b), the point mass intensity has been determined by increasing continuously the parameter m until the abscissa $s(P_{2l}(m))$ (which is moving to the left, see Fig. 4) reaches the abscissa $s(P_1(m))$ (which is moving to the left too). Numerical results confirm that this choice improves the accuracy of the identification and makes the estimate of m more stable.

The application of the identification algorithm requires the determination of the λ-s curves for continuously varying values of the parameter m. It can be shown that the results of identification depend on the size of the incremental mass step Δm, particularly in the transition between case 2a and case 2b. A refined numerical analysis has been developed on this issue in order to obtain accurate estimates with a reasonable computational effort. In the actual version, we have followed a search strategy divided in two steps, both of them based on the above-mentioned methodology, but with different Δm values. In a first stage, corresponding to the first iterations, we have adopted $\Delta m_1 = k_1 m_1^-$ (case 1) and $\Delta m_2 = k_2 m_2^-$ (cases 2a and 2b), where k_1 and k_2 are two positive numbers (less than 1) to be chosen by the user. In the second step, we have applied a constant incremental step Δm_f. In our experience, good choices are $k_1 = \frac{1}{20}, k_2 = \frac{1}{10}$ and $\Delta m_f = 10^{-5}$ for all the case studied. A flow-chart of the code and details on its numerical implementation are presented in Fig. 8.

The identification algorithm has been implemented on a computer with an Intel(R) Core (TM) i3 2.53 GHz processor and 4 GB of RAM, and a standard numerical code written in Matlab environment has been used to solve the eigenvalue problem (168) and to build the reconstruction procedure.

9.3. Results of numerical tests

The identification algorithm has been applied to a large variety of rod profiles, with different intensity and position of the point mass. A selected, but representative, series of results is presented here for rods with (normalized) cross-sectional area $a = a(x)$ given by

$$a_S(x) = 0.8 - 0.2\sin(3\pi x) \quad \text{(sinusoidal profile)}, \tag{176}$$

$$a_P(x) = 0.8(1 + x - x^2) \quad \text{(parabolic profile)}, \tag{177}$$

$x \in [0, 1]$.

The approximating eigenvalue problem (168) was defined by dividing the interval $[0, 1]$ into 200 equally spaced finite elements. The choice of the mesh-size guarantees negligible errors on the estimate of the first two (positive) natural frequencies of the rod. The computing time for each identification ranges from 8.7 s ($s = 0.48$, $m = 0.001$, parabolic profile) to 425.3 s ($s = 0.43$, $m = 0.25$, sinusoidal profile), and the average time corresponding to the eighty cases considered was 99.4 s.

The results of identification in absence of errors are show in Tables 1,2. It can be seen that the agreement between identified and actual values of the damage parameters is very good. Some discrepancy appears in the case of cracks with small severity (i.e., small m) and located close to the end of the rod. Maximum errors are of one-two points percent, and usually they arise for damage positions corresponding to a transition between the subcases (a) and (b) of the second case in the reconstruction algorithm.

All the results collected in Tables 1,2 were obtained by using the following incremental steps: $\Delta m_1 = \frac{m_1^-}{20}$ (case 1), $\Delta m_2 = \frac{m_2^-}{10}$ (cases 2a and 2b), $\Delta m_f = 10^{-5}$.

Once the point mass intensity m and its location s have been identified, it is possible to recover the crack depth, provided that an explicit relationship between the crack depth and the stiffness K is known. As an example, let us consider a steel rod with rectangular cross-section, of side $B = const$, height $H = H(z)$ and area $\hat{A}(z) = BH(z)$, which contains a pair of symmetric open edge cracks, each with front parallel to the side B, at the cross-section of abscissa z_d. Denoting by $\frac{d}{2}$ the depth of each side crack, the stiffness $\hat{K}$ of the elastic spring simulating the damage is expressed as

$$\hat{K} = \frac{E\hat{A}(z_d)}{L\delta_l(\nu;\alpha)}, \tag{178}$$

where (see Ruotolo and Surace (2004))

$$\delta_l(\nu;\alpha) = 2\frac{H(z_d)}{L}(1-\nu^2)(0.7314\alpha^8 - 1.0368\alpha^7 + 0.5803\alpha^6 + 1.2055\alpha^5 - 1.0368\alpha^4 + 0.2381\alpha^3 + 0.9852\alpha^2) \tag{179}$$

and $\alpha = \frac{d}{H(z_d)}$ is the crack ratio. Therefore, from the identified values of m and s, by knowing $\frac{H(z_d)}{L}$ and using (13), it is possible, first, to determine $\delta_l(\nu;\alpha)$ and, next, the crack depth d by inverting Eq. (179) with respect to α. For usual values of ν (e.g., $\nu \simeq 0.3$), the function $\delta_l = \delta_l(\nu;\cdot)$ is always uniquely invertible in the interval $\alpha \in [0, 1]$, but the interval in which expression (179) is accurate is usually smaller.

9.4. Applications to experimental data

In order to evaluate the stability of the method in presence of experimental/modeling errors on the data, a series of experiments were carried out. In particular, two applications shall be examined in detail in the sequel.

The mechanical model of Test 1 is a free–free steel rod of length $L = 2.925$ m and square solid cross-section 22×22 mm, with axial stiffness and linear mass density equal to $E\hat{A} = 9.9491 \cdot 10^7$ N and $\rho = 3.735$ kg/m, respectively. The rod has been damaged at the cross-section located at $z_d = 1.000$ m from one end ($s = z_d/L = 0.34$), see Fig. 9. Three different damage configurations, D1, D2 and D3, were obtained by introducing a notch of increasing depth. Details of the experimental setup and of the experimental modal analysis results can be found in Morassi (2001). In brief, the rod was suspended by two steel wire ropes to simulate free-free boundary conditions. The excitation was introduced at one end by means of an impulse force hammer, while the axial response was measured by a piezoelectric accelerometer fixed in the centre of an end cross-section of the rod. Vibration signals were acquired by a dynamic analyser and then processed in the frequency domain to measure the relevant frequency response term (inertance). The well-separated vibration modes and the very small damping allowed identification of the natural frequencies by means of the single mode technique.

Table 3 compares the experimental natural frequencies and their corresponding analytical estimates for the undamaged and

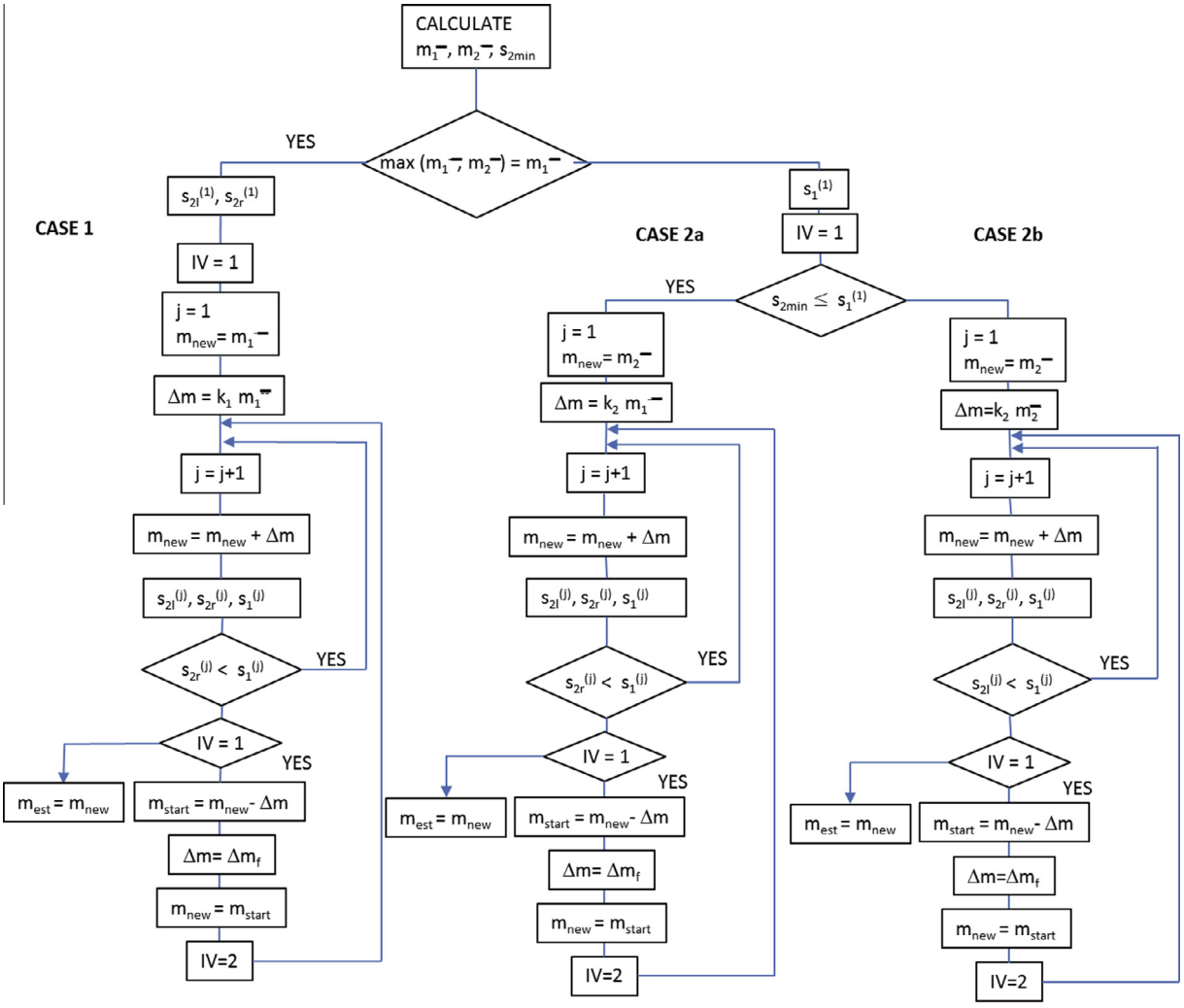

Fig. 8. Flow-chart of the identification algorithm.

Table 1
Identification of the mass intensity m and position s in a free–free non-uniform rod with the sinusoidal profile given in (176), by the first two (positive) natural frequencies. Percentage errors: $e_m = 100 \times (m_{est} - m)/m$, $e_s = 100 \times (s_{est} - s)/s$.

Position s	$m = 0.001$			$m = 0.010$			$m = 0.100$			$m = 0.250$		
	e_m	e_s	Case	e_m	e_s	Case	e_m	e_s	Case	e_m	e_s	Case
0.03	0.56	−0.31	2b	0.08	−0.05	2b	0.01	0.00	2b	0.00	0.00	2b
0.08	0.56	−0.34	2b	0.01	0.00	2b	0.01	0.00	2b	0.00	0.00	2b
0.13	0.37	−0.27	2b	0.05	−0.04	2b	0.01	−0.01	2b	0.00	0.00	2b
0.18	0.76	−0.77	2b	0.09	−0.09	2b	0.00	−0.01	2b	0.00	−0.01	2b
0.23	0.84	−1.94	2b	0.00	−0.18	2b	0.01	−0.05	2b	0.00	0.01	2a
0.28	0.89	1.63	2a	0.09	0.17	2a	0.00	0.01	2a	0.00	0.00	2a
0.33	0.21	0.10	2a	0.00	0.00	2a	0.01	0.00	2a	0.00	0.00	1
0.38	0.35	0.07	1	0.05	0.01	1	0.01	0.00	1	0.00	0.00	1
0.43	0.17	0.02	1	0.05	0.00	1	0.01	0.00	1	0.00	0.00	1
0.48	0.53	0.01	1	0.04	0.00	1	0.00	0.00	1	0.00	0.00	1

damaged rod. For the definition of the analytical model for the damaged rod, the theoretical value of the stiffness $\hat{K}$, for each damage configuration, was obtained by assuming that the position of the damage is known and by taking the measured value for the fundamental (positive) frequency of the damaged rod. Thus, the actual values of $\hat{K}$ for the different damage configurations are the following: $\hat{K} = 3.09119 \times 10^{10} N/m$ (case D1, corresponding to $m = K^{-1} = 0.0011$), $\hat{K} = 7.84984 \times 10^{9} N/m$ (case D2, $m = 0.0043$), $\hat{K} = 4.37183 \times 10^{8} N/m$ (case D3, $m = 0.0780$). The analytical model turns out to be extremely accurate for all the configurations under investigation and the discrepancy between measured and analytical values of the first two positive natural frequencies is lower than 0.04 per cent. Frequency shifts induced by the damage are significantly larger than the modeling errors, and are about $0.08, 0.32, 5$ per cent of the undamaged value for damage configurations $D1, D2$ and $D3$, respectively. Table 4 shows the estimated

Table 2
Identification of the mass intensity m and position s in a free–free non-uniform rod with the parabolic profile given in (177), by the first two (positive) natural frequencies. Percentage errors: $e_m = 100 \times (m_{est} - m)/m$, $e_s = 100 \times (s_{est} - s)/s$.

Position s	$m = 0.001$			$m = 0.010$			$m = 0.100$			$m = 0.250$		
	e_m	e_s	Case	e_m	e_s	Case	e_m	e_s	Case	e_m	e_s	Case
0.03	0.76	−0.41	2b	0.04	−0.02	2b	0.00	0.00	2b	0.00	0.00	2b
0.08	0.17	0.09	2b	0.04	−0.02	2b	0.01	−0.01	2b	0.00	0.00	2b
0.13	0.33	−0.20	2b	0.02	−0.01	2b	0.01	−0.01	2b	0.00	0.00	2b
0.18	0.76	−0.63	2b	0.06	−0.05	2b	0.00	0.00	2b	0.00	0.00	2b
0.23	0.44	−0.84	2b	0.07	−0.14	2b	0.01	−0.07	2b	0.00	0.01	2a
0.28	0.56	0.89	2a	0.00	0.00	2a	0.00	0.00	2a	0.00	0.00	2a
0.33	0.76	0.34	2a	0.06	0.02	2a	0.00	0.00	1	0.00	0.00	1
0.38	0.17	0.03	1	0.01	0.00	1	0.00	0.00	1	0.00	0.00	1
0.43	0.58	0.05	1	0.07	0.01	1	0.01	0.00	1	0.00	0.00	1
0.48	0.57	0.01	1	0.08	0.00	1	0.01	0.00	1	0.00	0.00	1

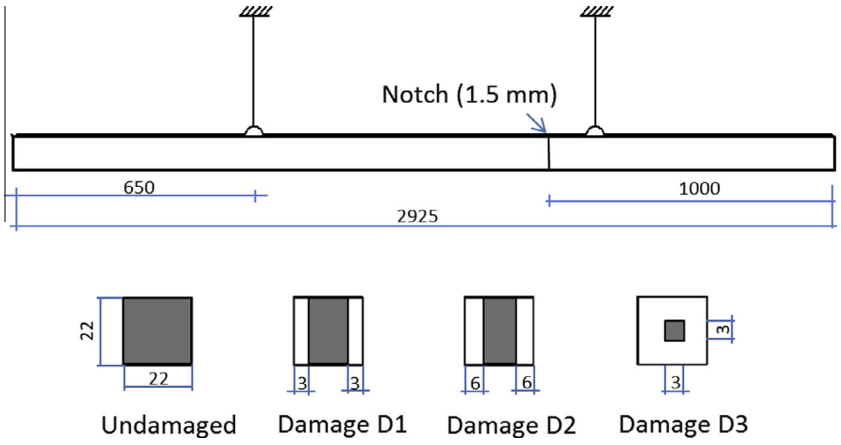

Fig. 9. Experimental specimen of Test 1. Lengths in mm.

values of the normalized position s of the cracked section and the spring stiffness K. The agreement with the theory is very good.

Test 2 is based on the experimental results presented in Dilena and Morassi (2004). The mechanical model is a double T free–free steel rod of series HE100B. The length is $L = 2.747$ m, the linear mass density is $\rho = 20.4$ kg/m and $E\hat{A} = 5.454 \cdot 10^8$ N. The damage was obtained by saw cutting the rod at the cross-section at $z_d = 0.550$ m ($s = z_d/L = 0.2002$) far from the left end, see Fig. 10. Two different damage configurations, called D4 and D5 in the following, were obtained by introducing a notch of increasing depth. Details of the experimental setup and discussion on the results of experimental modal analysis can be found in Dilena and Morassi (2004).

Table 5 compares the experimental values of the first two (positive) natural frequencies with their corresponding analytical estimates, both for the undamaged and damaged rod. The actual value of the spring stiffness $\hat{K}$ of the cracked rod was defined by assuming the position of the damage as known and providing that, for each damage configuration, the measured and the analytical fundamental (positive) natural frequency coincide. Thus, the actual values for the different damage configurations are the following: $\hat{K} = 3.507 \times 10^{10}$ N/m (case D4, $m = 0.0057$), $\hat{K} = 1.736 \times 10^9$ N/m (case D5, $m = 0.1140$). Frequency shifts induced by damage in the first two resonances are around 0.2–0.6 and 4–10 per cent for configuration D4 and D5, respectively. As modeling errors are concerned, the analytical model turns out to be accurate for natural

Table 4
Identification results in Test 1: actual values (s, m) versus estimated values (s_{est}, m_{est}). Percentage errors in brackets: $100 \times (s_{est} - s)/s$, $100 \times (m_{est} - m)/m$. t = computing time (in seconds).

	D1	D2	D3
s	0.34	0.34	0.34
m	0.0011	0.0043	0.078
s_{est}	0.3495 (2.79)	0.3384 (−0.47)	0.3411 (0.32)
m_{est}	0.0011 (0.00)	0.0044 (2.33)	0.078 (0.00)
t	13.59	17.99	66.98

Table 3
Test 1: First two positive natural frequencies $f_n = \frac{\omega_n}{2\pi}, n = 1, 2$, (expressed in Hz) of the undamaged free–free rod and their values associated to damage configurations $D_i, i = 1, 2, 3$. Note: Modeling errors Δ are reported in brackets, $\Delta = 100 \times (f_n^{Model} - f_n^{Exp})/f_n^{Exp}$.

	Undamaged		D1		D2		D3	
	Exp.	Model	Exp.	Model	Exp.	Model	Exp.	Model
f_1	882.25 (0.00)	882.25	881.5 (0.00)	881.5	879.3 (0.00)	879.3	831.0 (0.00)	831.0
f_2	1764.6 (-0.006)	1764.5	1763.3 (−0.011)	1763.1	1759.0 (0.011)	1759.2	1679.5 (0.036)	1680.1

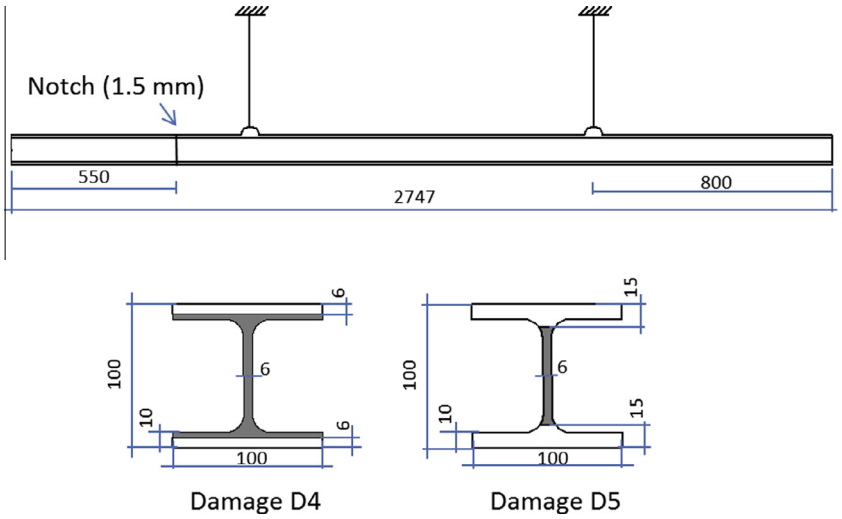

Fig. 10. Experimental specimen of Test 2. Lengths in mm.

Table 5
Test 2: First two positive natural frequencies $f_n = \frac{\omega_n}{2\pi}, n = 1, 2$, (expressed in Hz) of the undamaged free–free rod and their values associated to damage configurations $D_i, i = 1, 2, 3$. Note: Modeling errors Δ are reported in brackets, $\Delta = 100 \times (f_n^{Model} - f_n^{Exp})/f_n^{Exp}$.

	Undamaged		D4		D5	
	Exp.	Model	Exp.	Model	Exp.	Model
f_2	941.1 (0.00)	941.1	939.3 (0.00)	939.3	901.8 (0.00)	901.8
f_3	1879.1 (0.16)	1882.2	1868.3 (0.23)	1872.5	1693.3 (0.25)	1697.6

Table 6
Identification results in Test 2: actual values (s, m) versus estimated values (s_{est}, m_{est}). Percentage errors in brackets: $100 \times (s_{est} - s)/s, 100 \times (m_{est} - m)/m$. t = computing time (in seconds).

	D4		D5	
	Exp.	Pseudo-exp.	Exp.	Pseudo-exp.
s	0.2002	0.2002	0.2002	0.2002
m	0.0057	0.0057	0.1140	0.1140
s_{est}	0.0937 (−53.20)	0.1964 (−1.90)	0.1961 (−2.05)	0.2004 (+0.10)
m_{est}	0.0231 (+305.26)	0.0059 (3.51)	0.1183 (3.77)	0.1144 (+0.35)
t	54.64	23.41	132.74	125.36

frequencies, with maximum differences between experimental and theoretical values equal to 0.25 per cent. Therefore, although the analytical model can be considered accurate, percentage crack-induced changes in natural frequencies are comparable with the accuracy of the rod model for damage level D4.

Table 6 collects the estimated values of the position of the cracked section and the spring stiffness. The agreement for configuration D5 is good, whereas, as expected, the inaccuracy of the data prejudices the reliability of the reconstruction for configuration D4. Estimates are definitively better in case D4 if experimental data are replaced by pseudo-experimental data, namely, if the first two natural frequencies are determined by the analytical model of cracked rod, as it is shown in Table 5.

10. Conclusions

The inverse problem of identifying a single crack in a longitudinally vibrating rod by minimal frequency data has been considered in this paper. The rod profile is assumed to be a smooth function, symmetric with respect to the mid-point of the rod axis. The crack is assumed to remain open during vibration and it is modeled by a massless translational linearly elastic spring located at the damaged cross-section. No assumption on the smallness of the crack severity has been imposed.

We proved that the crack can be uniquely identified, up to a symmetric position, by the first two positive resonant frequencies of the damaged rod under free–free end conditions. Moreover, it was shown that the measurement of the first positive resonant frequency and the first antiresonant frequency of the frequency response evaluated at one end of the rod allows for a unique identification of the crack.

The proof is constructive, e.g., leads to a constructive identification procedure, and it is based on a careful analysis of the eigenvalues as functions of the damage position and damage intensity. The results of a series of numerical simulations show a good agreement with the theory. Applications of the method to experimental data also yields satisfactory identification, provided that modeling/noise errors are less than crack-induced changes on the frequency data.

Concerning possible generalizations of the proposed damage identification method, it is expected that the present results can hold also for rods with non-symmetric profile. The main difficulty here is due to the fact that the proof of Theorem 5.5 (and Theorem 8.1) cannot be directly extended to cover the non-symmetric case. A further line of investigation which is still open, and which is important for applications, consists in identifying a single open crack in a non-uniform beam under in-plane bending vibrations. In this case, the crack is modeled by the insertion of a massless rotational spring located at the damaged cross-section. Some of the mathematical tools we have adopted in the treatment of the longitudinal vibrations have no straightforward generalization to the bending case, and a preliminary analysis suggests that a different approach will be necessary to deal with this challenging diagnostic problem. Moreover, it is expected that appropriate numerical methods, such as those proposed in Low (1993), Tang (2003) and Xu et al. (2014), should be adopted in the bending case in order to ensure high accuracy in eigenfrequency and eigenfunction estimates.

Acknowledgement

The work of A. Morassi is supported by the University Carlos III of Madrid-Banco de Santander Chairs of Excellence Programme for the 2013–2014 Academic Year.

A. Morassi wishes to thank the colleagues of the University Carlos III of Madrid, especially Professors L. Rubio and J. Fernández-Sáez, for the warm hospitality at the Department of Engineering Mechanics.

The authors are grateful to Professor Giovanni Alessandrini for providing a proof of the eigenvalue derivative (32).

Appendix A

The present section is devoted to the proofs of some technical result we have used throughout the paper.

A.1. Proof of Proposition 3.1

Let $y = y(x,\lambda)$ be the unique solution to the initial value problem

$$\begin{cases} (by')' + \lambda by = 0, \quad x \in (0,s)\cup(s,1), & (180)\\ y(0) = 0, & (181)\\ y'(0) = 1, & (182)\\ [[y(s)]] = 0, & (183)\\ [[by'(s)]] = -\lambda m y(s), & (184)\end{cases}$$

for $\lambda \in \mathbb{R}$. The eigenvalues of (14)–(17) are the zeros of the equation $y(1,\lambda) = 0$. To prove the result it is enough to show that $\frac{dy(1,\lambda)}{d\lambda}|_{\lambda=\lambda_n} \neq 0$ for every $n = 1,2,\ldots$. We take the derivative of the differential Eq. (180) with respect to λ, multiply by y and integrate by parts on $(0,1)$, obtaining

$$b(1)\dot{y}'(1,\lambda)y(1,\lambda) + my^2(s,\lambda) + \lambda m y(s,\lambda)\dot{y}(s,\lambda) - \int_0^1 b\dot{y}'y' + \int_0^1 by^2 + \lambda\int_0^1 by\dot{y} = 0, \tag{185}$$

where $\dot{y} = \frac{dy}{d\lambda}$. Similarly, we multiply (180) by $\dot{y}$ and integrate by parts on $(0,1)$, obtaining

$$b(1)y'(1,\lambda)\dot{y}(1,\lambda) + \lambda m y(s,\lambda)\dot{y}(s,\lambda) - \int_0^1 by'\dot{y}' + \lambda\int_0^1 by\dot{y} = 0. \tag{186}$$

Subtracting (186) from (185) and taking $\lambda = \lambda_n$ we have

$$b(1)y'(1,\lambda_n)\dot{y}(1,\lambda_n) = my^2(s,\lambda_n) + \int_0^1 by^2(x,\lambda_n)dx. \tag{187}$$

Clearly, $y'(1,\lambda_n) \neq 0$ (e.g., if $y'(1,\lambda_n) = 0$, then $y(x,\lambda_n) \equiv 0$ in $[0,1]$, a contradiction) and the right hand side of (187) is strictly positive. Then, $\dot{y}(1,\lambda_n) \neq 0$.

A.2. Proof of Proposition 3.3

We start by showing that the first eigenfunction w_1 (associated to the eigenvalue λ_1) of (14)–(17) has no zeros in $(0,1)$. We adapt a method by Weinberger (1965). By the variational formulation of the eigenvalue problem (26), we have

$$\lambda_1 = \min_{\varphi\in H_0^1(0,1)\setminus\{0\}} R[\varphi] = R[w_1], \quad R[\varphi] = \frac{\int_0^1 b(\varphi')^2}{m\varphi^2(s) + \int_0^1 b\varphi^2}. \tag{188}$$

If w_1 is the eigenfunction associated to λ_1, then also $|w_1|$ is an eigenfunction associated to λ_1. By Corollary 3.2 we have

$$|w_1(x)| = cw_1(x), \quad x \in [0,1], \tag{189}$$

with c constant such that $|c| = 1$. In particular, if $c = 1$ then $w_1(x) \geqslant 0$ in $[0,1]$, and if $c = -1$ then $w_1(x) \leqslant 0$ in $[0,1]$. Suppose that $c = 1$ (one can proceed analogously if $c = -1$.) Assume that there exists a point $x_0, 0 < x_0 < 1$, such that $w_1(x_0) = 0$. Then, since $w_1(x) \geqslant 0$ in $[0,1]$, we have $w_1'(x_0) = 0$, that is $w_1(x) \equiv 0$ in $[0,1]$, a contradiction.

To proceed with higher order eigenfunctions, we need the following result, which is a generalization of the well-known Sturm–Liouville result when $m = 0$.

Lemma 10.1. *Let $\lambda, \mu \in \mathbb{R}$ and let $s, a_1, a_2 \in \mathbb{R}$ such that $-\infty < a_1 < s < a_2 < \infty$. Let u, v be two nontrivial real-valued solutions to*

$$\begin{cases} (bu')' + \lambda bu = 0, \quad x \in (a_1,s)\cup(s,a_2), & (190)\\ [[u(s)]] = 0, & (191)\\ [[bu'(s)]] = -\lambda m u(s), & (192)\end{cases}$$

$$\begin{cases} (bv')' + \mu bv = 0, \quad x \in (a_1,s)\cup(s,a_2), & (193)\\ [[v(s)]] = 0, & (194)\\ [[bv'(s)]] = -\lambda m v(s). & (195)\end{cases}$$

Suppose that $\mu > \lambda$ and suppose that x_1, x_2 are two consecutive zeros of $u, a_1 \leqslant x_1 < x_2 \leqslant a_2$. Then, there exists $\bar{x} \in (x_1,x_2)$ such that $v(\bar{x}) = 0$.

Proof. If $s \in \mathbb{R}\setminus(x_1,x_2)$, then the thesis follows from classical results, see, for example, Titchmarsh (1962). Then, let us take s such that $x_1 < s < x_2$. We multiply (190) by v and (193) by u, and we integrate by parts in (x_1,x_2). Taking into account the jump conditions at $x = s$, we have

$$0 = b(x_2)u'(x_2)v(x_2) - b(x_1)u'(x_1)v(x_1) + \lambda m u(s)v(s) - \int_{x_1}^{x_2} bu'v' + \lambda\int_{x_1}^{x_2} buv, \tag{196}$$

$$0 = \mu m u(s)v(s) - \int_{x_1}^{x_2} bu'v' + \mu\int_{x_1}^{x_2} buv. \tag{197}$$

Subtracting (197) from (196) we obtain

$$b(x_2)u'(x_2)v(x_2) - b(x_1)u'(x_1)v(x_1) = (\mu-\lambda)mu(s)v(s) + (\mu-\lambda)\int_{x_1}^{x_2} buv. \tag{198}$$

Suppose that $u(x) < 0$ in (x_1,x_2). Then, $u'(x_1) > 0$ and $u'(x_2) < 0$ (since the zeros of the eigenfunctions are simple, see Proposition 3.1). If v does not vanish in (x_1,x_2), then either $v > 0$ in (x_1,x_2) or $v < 0$ in (x_1,x_2). If $v > 0$ in (x_1,x_2), then the left hand side of (198) is negative, whereas the right hand side is positive, a contradiction. Similarly, if $v < 0$ in (x_1,x_2). Therefore, v must change of sign inside (x_1,x_2). Note that we have the same conclusion if $s = x_1$ or $s = x_2$. □

Let us recall without proof the following classical result.

Lemma 10.2. *Let $s \in (0,1)$ and consider nontrivial solutions u, v to*

$$(bu')' + \lambda bu = 0, \quad x \in (0,s), \tag{199}$$

$$(bv')' + \mu bv = 0, \quad x \in (0,s), \tag{200}$$

with

$$u(0) = v(0) = 0, \quad \mu > \lambda. \tag{201}$$

If u has m zeros in $(0,c], m \geqslant 0$ and $c \leqslant s$, then v has at least m zeros in $(0,c]$, and the nth zero of v is less than the nth zero of u.

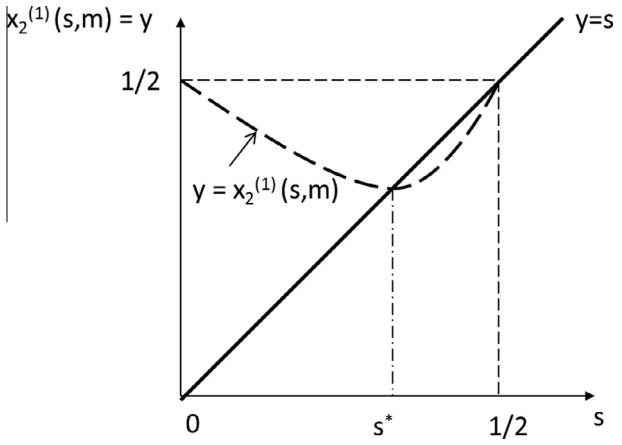

Fig. 11. On the proof of Proposition 10.5.

Remark 10.3. An analogous result holds if we replace the end condition (201) by $u(1) = v(1) = 0$ and if we count the zeros of u, v inside intervals $[c, 1), s \leqslant c$.

By the two above lemmas, we can estimate from below the number of zeros of an eigenfunction. In fact, we have the following result.

Lemma 10.4. *The nth eigenfunction w_n of (14)–(17) has at least $n-1$ zeros inside $(0,1), n \geqslant 2$.*

We are now in position to prove that the nth eigenfunction of (14)–(17), $n \geqslant 2$, has *exactly* $n-1$ zeros inside $(0,1)$.

We follow again the arguments in Weinberger (1965). Suppose that w_n has $l-1$ interior zeros at $0 = x_0 < x_1 < x_2 < \ldots < x_{l-1} < x - l = 1$, where $l - 1 \geqslant n - 1$ by Lemma 10.4, and define, for $m = 1, \ldots, l$, the functions

$$g^m(x) = \begin{cases} w_n(x), & x \in (x_{m-1}, x_m), \\ 0, & x \in [0,1] \setminus (x_{m-1}, x_m). \end{cases} \tag{202}$$

The function g^m belongs to $H_0^1(0,1) \setminus \{0\}$ and also the function $\varphi(x) = \sum_{m=1}^{l} c_m g^m(x)$ belongs to $H_0^1(0,1) \setminus \{0\}$, for every set of real constants $\{c_1, \ldots, c_l\}$. The l constants $\{c_i\}_{i=1}^{l}$, $(c_1, \ldots, c_l) \neq (0, \ldots, 0)$, can be chosen such that the following $l-1$ linear constraints are satisfied:

$$\int_0^1 b\varphi g^i + m\varphi(s) g^i(s) = 0, \quad i = 1, \ldots, l-1. \tag{203}$$

We assume, without loss of generality, that s belongs to the second interval (x_1, x_2). Integrating by parts, we obtain

$$\begin{aligned} \int_0^1 b\varphi'^2 &= \sum_{m=1}^{l} c_m^2 \int_{x_{m-1}}^{x_m} b(w_n')^2 = c_1^2 \left[bw_n' w_n|_{x_0}^{x_1} + \int_{x_0}^{x_1} (-(bw_n')' w_n) \right] \\ &\quad + c_2^2 \left[bw_n' w_n|_{x_1}^{s^-} + bw_n' w_n|_{s^+}^{x_2} + \int_{x_1}^{x_2} (-(bw_n')' w_n) \right] \\ &\quad + c_3^2 \left[bw_n' w_n|_{x_2}^{x_3} + \int_{x_2}^{x_3} (-(bw_n')' w_n) \right] + \ldots \\ &= \lambda_n c_1^2 \int_{x_0}^{x_1} bw_n^2 + \lambda_n c_2^2 \left(mw_n^2(s) + \int_{x_1}^{x_2} bw_n^2 \right) \\ &\quad + \lambda_n c_3^2 \int_{x_2}^{x_3} bw_n^2 + \ldots = \lambda_n \left(m\varphi^2(s) + \int_0^1 b\varphi^2 \right), \end{aligned} \tag{204}$$

that is

$$\lambda_n = R[\varphi]. \tag{205}$$

By the variational characterization of the eigenvalues (26), for such a φ we have $R[\varphi] \geqslant \lambda_l$. Then, by (205), $\lambda_n = R[\varphi] \geqslant \lambda_l$, that is $n \geqslant l$. But, by Lemma 10.4, we already know that $l \geqslant n$. Therefore, we must have $l = n$, which is the thesis stated in Proposition 3.3.

A.3. Proof of Proposition 10.5

The following technical result has been used in the proof of Theorem 5.5 (Case (ii)).

Proposition 10.5. *Let $b \in C^1([0,1])$ and $b(x) = b(1-x)$ in $[0,1]$. Let $s \in (0, \frac{1}{2})$ and $0 < m < \infty$. The zero of the second eigenfunction w_2 of (14)–(17), say $x_2^{(1)}$, is such that*

$$s < x_2^{(1)} < \frac{1}{2}. \tag{206}$$

Proof. By Proposition 5.3, we have $w_2^U(s) \neq 0$ and then, by Proposition 5.2, the node of w_2 moves toward the point mass, namely $x_2^{(1)} < \frac{1}{2}$. It remains to prove that $s < x_2^{(1)}$. To prove this statement, we can imagine to move continuously the mass m from the left end ($x = 0$) to the right, toward the mid-span of the rod. By moving the mass, the node $x_2^{(1)} = x_2^{(1)}(s,m)$ of the mode w_2 will stay inside the interval $(0, \frac{1}{2})$ (since, by Proposition 5.2, the node moves from the referential position $\frac{1}{2}$ toward the position of the mass). If $x_2^{(1)}(s,m) > s$ for every $s \in (0, \frac{1}{2})$, there is nothing to prove. Suppose, on the contrary, that $x_2^{(1)}(s,m) < s$ for some $s \in (0, \frac{1}{2})$, see Fig. 11 (dashed curve). Then, by continuity, there exists $s^* \in (0, \frac{1}{2})$ such that $x_2^{(1)}(s^*, m) = s^*$, that is $w_2(s^*; s^*) = 0$. But, by Proposition 5.1, this implies $w_2^U(s^*) = 0$, which is a contradiction since the only zero of w_2^U is at $x = \frac{1}{2}$ and $s^* < \frac{1}{2}$. It follows that $s < x_2^{(1)}$ for every $s \in (0, \frac{1}{2})$, and the proof is complete. □

References

Adams, R.D., Cawley, P., Pye, C.J., Stone, B.J., 1978. A vibration technique for non-destructively assessing the integrity of structures. J. Mech. Eng. Sci. 20 (2), 93–100.

Brezis, H., 1986. Analisi Funzionale. Liguore Editore, Napoli, Italy.

Cabib, E., Freddi, L., Morassi, A., Percivale, D., 2001. Thin notched beams. J. Elasticity 64 (2/3), 157–178.

Caddemi, S., Morassi, A., 2013. Multi-cracked Euler–Bernoulli beams: mathematical modelling and exact solutions. Int. J. Solids Struct. 50 (6), 944–956.

Cerri, M.N., Vestroni, F., 2000. Detection of damage in beams subjected to diffused cracking. J. Sound Vib. 234 (2), 259–276.

Chaudhari, T.D., Maiti, S.K., 2000. A study of vibration of geometrically segmented beams with and without crack. Int. J. Solids Struct. 37, 761–779.

Courant, R., Hilbert, D., 1966. Methods of Mathematical Physics (volume I). Interscience Publishers Inc., New York (First English Edition).

Dilena, M., Morassi, A., 2004. The use of antiresonances for crack detection in beams. J. Sound Vib. 276 (1–2), 195–214.

Freund, L.B., Herrmann, G., 1976. Dynamic fracture of a beam or plate in plane bending. J. Appl. Mech., 112–116, 76-APM-15

Gladwell, G.M.L., 2004. Inverse Problems in Vibration. Kluwer Academic Publishers, Dordrecht, The Netherlands, Second edition.

Gladwell, G.M.L., Morassi, A., 1999. Estimating damage in a rod from changes in node positions. Inverse Prob. Eng. 7 (3), 215–233.

Lin, H.-P., Chang, S.-C., 2004. Identification of crack location in a rod from measurements of natural frequencies, Preprint.

Liang, R.Y., Hu, J., Choy, F., 1992. Theoretical study of crack-induced eigenfrequency changes on beam structures. J. Eng. Mech. ASCE 118 (2), 384–396.

Low, K.H., 1993. A reliable algorithm for solving frequency equations involving transcendental functions. J. Sound Vib. 161 (2), 369–377.

Morassi, A., 1993. Crack-induced changes in eigenparameters of beam structures. J. Eng. Mech. ASCE 119 (9), 1798–1803.

Morassi, A., 2001. Identification of a crack in a rod based on changes in a pair of natural frequencies. J. Sound Vib. 242 (4), 577–596.

Morassi, A., Dilena, M., 2002. On point mass identification in rods and beams from minimal frequency measurements. Inverse Prob. Eng. 10 (3), 183–201.

Narkis, Y., 1994. Identification of crack location in vibrating simply supported beams. J. Sound Vib. 172 (4), 549–558.

Rubio, L., 2009. An efficient method for crack identification in simply supported Euler–Bernoulli beams. J. Vib. Acoust. 131, Paper 051001.
Rubio, L., Fernández-Sáez, J., Morassi, A., 2015. The full nonlinear crack detection problem in uniform vibrating rods. J. Sound Vib. 339, 99–111.
Ruotolo, R., Surace, C., 2004. Natural frequencies of a bar with multiple cracks. J. Sound Vib. 272, 301–316.
Springer, W.T., Lawrence, K.L., Lawley, T.J., 1988. Damage assessment based on the structural frequency-response function. Exp. Mech. 28 (1), 34–37.
Tang, Yu., 2003. Numerical evaluation of uniform beam modes. J. Eng. Mech. ASCE 129 (12), 1475–1477.
Titchmarsh, E.C., 1962. Eigenfunction Expansion Associated with Second-Order Differential Equations, Part I. Clarendon Press, Oxford, UK.
Vestroni, F., Capecchi, D., 2000. Damage detection in beam structures based on frequency measurements. J. Eng. Mech. ASCE 126, 761–768.
Weinberger, H.F., 1965. A First Course in Partial Differential Equations. Dover Publications Inc., New York, US.
Xu, W., Cao, M.S., Ren, Q.W., Su, Z.Q., 2014. Numerical evaluation of high-order modes for stepped beams. J. Vib. Acoust. Trans. ASME 136 (1), 014503.